Current Biology

Neural processing of the reward value of pleasant odorants

Highlights

- The posterior olfactory bulb is a site of intracranial self-stimulation

- Olfactory tubercle receives heavy projections from the posterior olfactory bulb

- Olfactory tubercle activity is related to odorant pleasantness in mice and humans

- Attractive odorants are natural rewards in both mice and humans

Authors

Maëllie Midroit, Laura Chalençon, Nicolas Renier, ..., Moustafa Bensafi, Anne Didier, Nathalie Mandairon

Correspondence

nathalie.mandairon@cnrs.fr

In Brief

Midroit et al. reveal that the odorants act as natural rewards. The olfactory tubercle gates olfactory information from the posterior olfactory bulb to the reward system to encode spontaneous odor-driven attraction.

CellPress

Current Biology

CellPress

Neural processing of the reward value of pleasant odorants

Maëllie Midroit,[1,2,3,9,10] Laura Chalençon,[1,2,3,10] Nicolas Renier,[4] Adrianna Milton,[5] Marc Thevenet,[1,2,3] Joëlle Sacquet,[1,2,3] Marine Breton,[1,2,3] Jérémy Forest,[1,2,3] Norbert Noury,[6] Marion Richard,[1,2,3] Olivier Raineteau,[7] Camille Ferdenzi,[1,2,3] Arnaud Fournel,[1,2,3] Daniel W. Wesson,[8] Moustafa Bensafi,[1,2,3] Anne Didier,[1,2,3] and Nathalie Mandairon[1,2,3,11,*]

[1]CNRS, UMR 5292, INSERM, U1028, Lyon Neuroscience Research Center, Neuroplasticity and Neuropathology of Olfactory Perception Team, Lyon 69000, France
[2]University Lyon, Lyon, 69000, France
[3]University Lyon 1, Villeurbanne 69000, France
[4]Sorbonne Universités, Paris Brain Institute, ICM, Inserm, CNRS, Paris, France
[5]Department of Neurosciences, Case Western Reserve University, 2109 Adelbert Road, Cleveland, OH 44106, USA
[6]CNRS, UMR5270, Institute Nanotechnology Lyon, Biomedical Sensors Group, University of Lyon 1, Villeurbanne 69621, France
[7]University Lyon, Université Claude Bernard Lyon 1, Inserm, Stem Cell and Brain Research Institute U1208, 69500 Bron, France
[8]Department of Pharmacology & Therapeutics, University of Florida, 1200 Newell Drive, Gainesville, FL 32610, USA
[9]Present address: Department of Fundamental Neurosciences, University of Lausanne, 1005 Lausanne, Switzerland
[10]These authors contributed equally
[11]Lead contact
*Correspondence: nathalie.mandairon@cnrs.fr
https://doi.org/10.1016/j.cub.2021.01.066

SUMMARY

Pleasant odorants are represented in the posterior olfactory bulb (pOB) in mice. How does this hedonic information generate odor-motivated behaviors? Using optogenetics, we report here that stimulating the representation of pleasant odorants in a sensory structure, the pOB, can be rewarding, self-motivating, and is accompanied by ventral tegmental area activation. To explore the underlying neural circuitry downstream of the olfactory bulb (OB), we use 3D high-resolution imaging and optogenetics and determine that the pOB preferentially projects to the olfactory tubercle, whose increased activity is related to odorant attraction. We further show that attractive odorants act as reinforcers in dopamine-dependent place preference learning. Finally, we extend those findings to humans, who exhibit place preference learning and an increase BOLD signal in the olfactory tubercle in response to attractive odorants. Thus, strong and persistent attraction induced by some odorants is due to a direct gateway from the pOB to the reward system.

INTRODUCTION

Since the dawn of time, we have flavored our dishes, perfumed our houses and ourselves. Our close relationship with smells exemplifies the strong attractive power odorants exert over us. Why do some odorants have such a strong power of attraction? Among the different dimensions of olfactory perception such as identity, intensity, or familiarity, the hedonic value (or pleasantness) dominates since it is the first criterion used by humans to describe and categorize odorants.[1–3] The hedonic value drives vital behaviors such as feeding, social relationships, and danger avoidance[4] and impacts a wide array of higher-order social functions in humans that contribute to our overall well-being.

The olfactory bulb (OB) is the first sensory structure for odor information processing.[5] We previously showed that in mice, pleasant odorants are represented in spatially restricted activity in the posterior olfactory bulb (pOB).[6] How does this hedonic information generate attraction to odor? Because motivated behaviors are known to rely on the reward/motivational system,[7–9] this question prompted us to explore the role of the reward system in odor-induced attraction.

Thus, using complementary approaches in mice and humans, we tested the hypothesis that pleasant odorants are attractive because they directly solicit the reward system.

First, we investigated whether activating the neural representation of pleasant odorants could be rewarding, and we found that optogenetic activation of pOB can serve as reinforcer using a self-stimulation paradigm, a widely used operant conditioning to assess the biological bases of motivation.[10,11] Second, we explored the underlying neural circuitry downstream of the OB and focused more particularly on the olfactory tubercle (OT), a direct target of the OB that is a component of the ventral striatum[12,13] and plays a role in motivated behaviors.[14–16] In this context, using 3D high-resolution imaging, electrophysiology, and cellular mapping and optogenetics, we deciphered the anatomical link between the pOB and the OT and revealed that stimulation of the pOB by spontaneously attractive odorants activates the OT and triggers motivated behaviors. Then, to further confirm the rewarding properties of odorants, we used a conditioned place preference test, a standard model used to evaluate the rewarding properties of drugs of abuse. This test showed that attractive odorants induced dopamine-dependent place preference learning. Finally, we extended
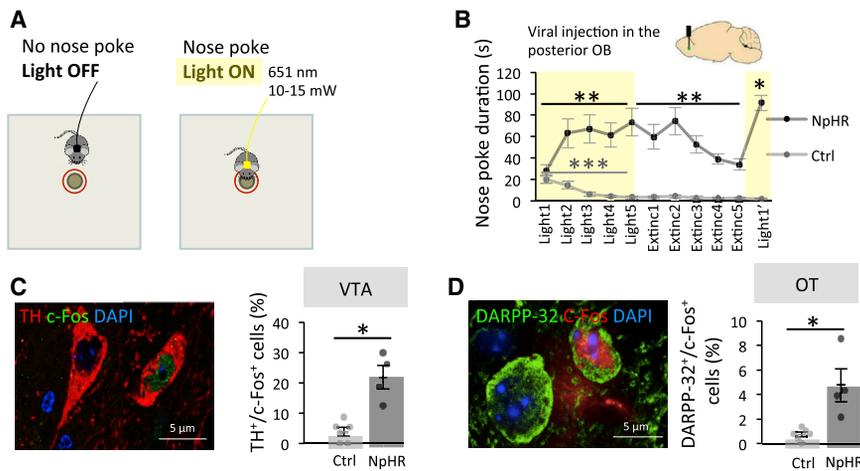
Figure 1. The pOB is a site for optogenetic intracranial self-stimulation

(A) Experimental setup.

(B) Top. Injection of NpHR-EYFP (NpHR n = 7) or control virus (Ctrl n = 9) in the posterior granule cell layer of the OB. Bottom. NpHR mice rapidly learned across days of learning to nose poke to trigger light-stimulation (Friedman test: trial effect $F_{(4,35)}$ = 13.60 p = 0.009, Two-Tailed Wilcoxon Light1 versus Light5 W = 28.000 p = 0.016, Rank-Biserial Correlation = 1.000). This learning was subject to extinction when light was no more available (Friedman test: trial effect $F_{(4,35)}$ = 20.31 p = 0.001, Two-Tailed Wilcoxon Light5 versus Extinc5 W = 27.000 p = 0.031, Rank-Biserial Correlation = 0.929). On the last trial, light was available again and nose poking reinstated (Two-Tailed Wilcoxon Extinc5 versus Light1' W = 28.000 p = 0.016, Rank-Biserial Correlation = 1.000). Nose pokes significantly decreased in Ctrl among the 5 first trials of light stimulation (Friedman trial effect $F_{(4,35)}$ = 21.36 p < 0.001, Two-Tailed Wilcoxon Light1 versus Light5 W = 36.000 p = 0.014, Rank-Biserial Correlation = 1.000). Values represent means ± SEM.

(C) Left. Representative image of double labeled TH+/c-Fos+ cells in the VTA. Right. The percentage of TH+ cells expressing c-Fos was higher in NpHR mice (n = 4) compared to Ctrl (n = 6) in the VTA after self-conditioning (Two-Tailed Mann-Whitney, W = 24.000 p = 0.014, Rank-Biserial Correlation = 1.000). Bars represent means of individual data points ± SEM.

(D) Left. Representative image of double labeled DARPP-32+/c-Fos+ cells in the OT. Right. The percentage of DARPP-32+ cells expressing c-Fos in OT was higher in NpHR (n = 4) mice compared to Ctrl (n = 6) after self-conditioning (Two-Tailed Mann-Whitney, W = 24.000 p = 0.014, Rank-Biserial Correlation = 1.000). Bars represent means of individual data points ± SEM *p < 0.05, **p < 0.01, ***p < 0.001.

See also Figure S1.

our findings to humans by identifying a similar recruitment of the reward system and more particularly of the olfactory tubercle by attractive odorants in humans, through both naturalistic living-lab experiments and functional brain imaging approaches.

RESULTS

The posterior olfactory bulb as a site for rewarding intracranial self-stimulation

Since optogenetic stimulation of the pOB increases attraction toward odorants,[6] we assessed whether this stimulation would by itself be sufficient to serve as a reinforcer and thus induce operant conditioning using optogenetic intracranial self-stimulation. Two groups of mice were injected with a Lenti-hSyn-eNpHR3.0-EYFP virus (NpHR-EYFP virus, NpHR group) or a control Lenti-hSyn-EYFP virus (EYFP virus, Ctrl group) in the ventro-posterior granule cell layer of the OB with optical fibers implanted at the same location (Figures 1A and 1B; Figures S1A and S1B). Light stimulation in NpHR mice silenced inhibitory granule interneurons as shown by a lower percentage of EYFP+/c-Fos+ neurons in the targeted part of the OB, showing that light stimulation inhibits NpHR transduced neurons (Figure S1C). This was not observed in Ctrl mice, showing that light alone had no effect on granule cell activity (Figure S1C). This manipulation was chosen since it leads to disinhibition/activation of OB projection neurons (mitral/tufted cells) specifically in the pOB.[6]

During behavior, bilateral light stimulation was automatically triggered when mice nose poked within 1 cm around a non-odorized hole of a board apparatus (light-triggering zone) and lasted as long as the nose poke (Figure 1A). Across days of training, we found that NpHR mice readily learned to nose poke to receive optogenetic stimulation in their pOB.

More precisely, the nose poke duration increased over the five days of training in NpHR mice (nose poke duration Light1 = 28.275 ± 5.469 s, Light5 = 73.697 ± 12.897 s; Friedman test: trial effect $F_{(4,35)}$ = 13.60 p = 0.009, Two-Tailed Wilcoxon Light1 versus Light5 W = 28.000 p = 0.016 Rank-Biserial Correlation = 1.000; Figure 1B) indicating that light stimulation serve as reinforcer in the operant conditioning paradigm. We then proceeded to an extinction phase during which light stimulation was no longer delivered upon nose poke (Trial 6 to Trial 10). During this second phase, NpHR mice showed a decrease in nose poke duration (nose poke duration Light5 = 73.697 ± 12.897 s, Extinc5 = 34.163 ± 5.286 s; Friedman test: trial effect $F_{(4,35)}$ = 20.31 p = 0.001, Two-Tailed Wilcoxon Light5 versus Extinc5 W = 27.000 p = 0.031 Rank-Biserial Correlation = 0.929; Figure 1B). Finally, in a third phase, light stimulation was available again, and a reinstatement of self-stimulation behavior was observed (nose poke duration Extinc5 = 34.163 ± 5.286 s, Light1' = 91.434 ± 7.114 s; Two-Tailed Wilcoxon Extinc5 versus Light1' W = 28.000 p = 0.016 Rank-Biserial Correlation = 1.000; Figure 1B). This learning/extinction/reinstatement sequence confirmed that self-stimulation behavior is dependent on optogenetic inhibition of granule cells in the pOB. This behavior was not observed in Ctrl mice (with no expression of NpHR in the granule cells), which instead showed a rapid and pronounced decrease in poke durations across trials regardless of light delivery (nose poke duration Light1 = 20.274 ± 4.074 s, Light5 = 3.222 ± 1.169 s; Friedman test: trial effect $F_{(4,35)}$ = 21.36 p < 0.001, Two-Tailed Wilcoxon Light1 versus Light5 W = 36.000 p = 0.014 Rank-Biserial Correlation = 1.000; Figure 1B). The difference between NpHR and Ctrl groups was observed at early as the second trial of light stimulation and remained over the five

Current Biology
Article

CellPress
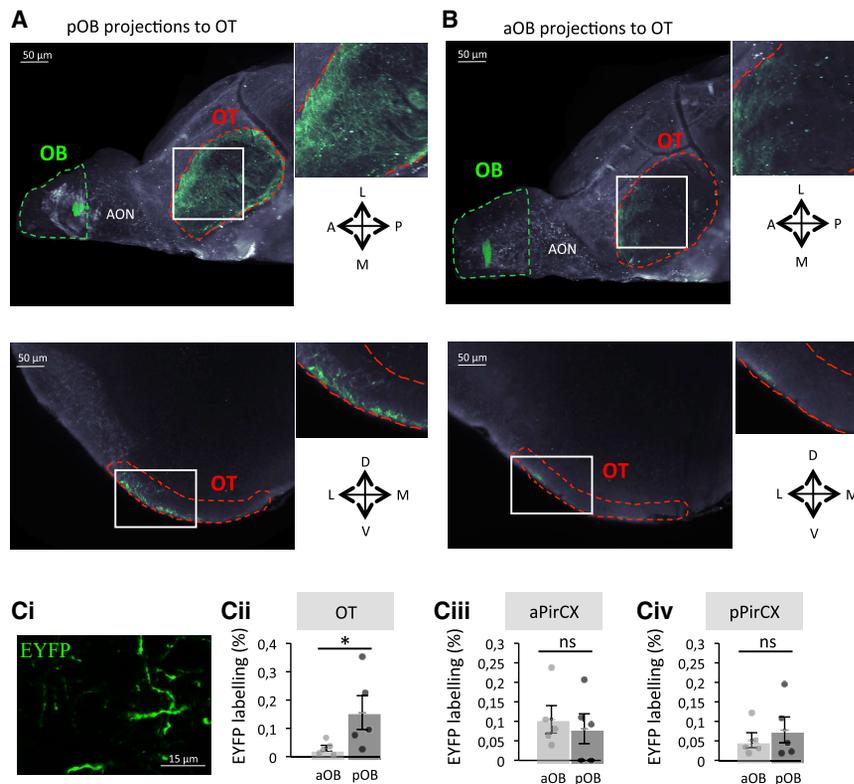
Figure 2. A privileged pathway exists between the pOB and the OT

(A) Representative image of the pOB projecting onto the OT after iDISCO clarification. Top. Ventral projection. Bottom. Coronal optical section.

(B) Representative image of the aOB projecting onto the OT after iDISCO clarification. Top. Ventral projection. Bottom. Coronal optical section.

(C) Quantification of the percentage of EYFP labeling (Ci, EYFP labeling = EYFP+area/total area of the field*100) after viral injections in the pOB (n = 5) and the aOB (n = 5) in the OT (Cii, Bonferroni corrected One-Tailed Mann-Whitney, W = 2.000 p = 0.048, Rank-Biserial Correlation = −0.840), aPirCX (Ciii, Bonferroni corrected One-Tailed Mann-Whitney, W = 14.000 p = 1, Rank-Biserial Correlation = 0.120) and pPirCX (Civ, Bonferroni corrected One-Tailed Mann-Whitney, W = 11.000 p = 1, Rank-Biserial Correlation = −0.120). Bars represent means of individual data points ± SEM *p < 0.05. A: Anterior; P: Posterior; L: Lateral; M: Medial; D: Dorsal; V: Ventral. See also Figure S2.

extinction trails revealing a rapid and persistent effect of the rewarding stimulation in NpHR mice (Bonferroni corrected One-Tailed Mann-Whitney, Light1 W = 43.000 p = 1 Rank-Biserial Correlation = 0.365, Light2 W = 61.000 p = 0.004 Rank-Biserial Correlation = 0.937, Light3 W = 63.000 p < 0.001 Rank-Biserial Correlation = 1.000, Light4 W = 63.000 p < 0.001 Rank-Biserial Correlation = 1.000, Light5 W = 63.000 p = 0.005 Rank-Biserial Correlation = 1.000, Extinc1 W = 63.000 p < 0.001 Rank-Biserial Correlation = 1.000, Extinc2 W = 63.000 p < 0.001 Rank-Biserial Correlation = 1.000, Extinc3 W = 63.000 p = 0.006 Rank-Biserial Correlation = 1.000, Extinc4 W = 63.000 p < 0.001 Rank-Biserial Correlation = 1.000, Extinc5 W = 63.000 p = 0.006 Rank-Biserial Correlation = 1.000, Light1' W = 63.000 p = 0.006 Rank-Biserial Correlation = 1.000). Moreover, we performed another set of experiments in mice which had NpHR-EYFP virus injected in their anterior OB (aOB) and were trained in the same behavioral protocol. NpHR mice injected in the aOB showed no increase in nose poking across trials (Light1-Light5) (nose poke duration Light1 = 7.835 ± 1.791 s, Light5 = 6.458 ± 2.466 s; Friedman test: trial effect $F_{(4,35)}$ = 5.90 p = 0.207; Figure S1D), indicating that self-stimulation behavior was specific to the stimulation of the pOB. In addition, on the first trial, NpHR aOB mice displayed less nose pokes than Ctrl mice (7.835 ± 1.791 versus 20.274 ± 4.074 s, when comparing Light1 trial in Figure S1D and Light1 trial Ctrl group in Figure 1B; Two-Tailed Mann-Whitney, W = 11.000 p = 0.015 Rank-Biserial Correlation = −0.694). This suggests an aversive effect of aOB granule cell inhibition in line with previous data by our group.[6] We verified the anterior location of the virus

injection and its efficiency by quantifying the activity of transduced cells after light stimulation (Figures S1E and S1F).

Next, to confirm that pOB self-stimulation recruits the reward system, we analyzed its impact on the activity of ventral tegmental area (VTA) dopaminergic neurons (TH+ cells) using assessment of c-Fos expression. We found a higher percentage of TH+/c-Fos+ double-labeled cells in light-stimulated NpHR mice injected in the pOB compared to the Ctrl group (TH+/c-Fos+ cells NpHR = 21.834 ± 3.888%, EYFP = 3.848 ± 1.392%; Two-Tailed Mann-Whitney, W = 24.000 p = 0.014 Rank-Biserial Correlation = 1.000; Figure 1C). Because the OT is at the crossroad between the OB and VTA, we further analyzed the activation of OT projection neurons, the medium spiny neurons (MSNs), identified based on DARPP-32+ expression.[17] We found a higher percentage of DARPP-32+/c-Fos+ cells in NpHR mice injected in the pOB compared to the Ctrl group (DARPP-32+/c-Fos+ cells NpHR = 4.758 ± 1.356%, EYFP = 0.735 ± 0.200%; Two-Tailed Mann-Whitney, W = 24.000 p = 0.014 Rank-Biserial Correlation = 1.000; Figure 1D), indicating the activation of a network including the OT and VTA after posterior bulbar self-stimulation.

Taken together, our results reveal that the pOB, but not the aOB, is a site of self-stimulation suggesting that the OT provides a direct gateway from the pOB to the reward system.

A privileged pathway between the posterior olfactory bulb and the olfactory tubercle

We next hypothesized that the capacity of the pOB to support reinforcement and to recruit the VTA could be due to an enrichment of the axonal projection densities between pOB and the OT, relative to aOB projections. To test this hypothesis, mice were injected with a lentivirus expressing EYFP in the mitral cell layer of aOB or pOB. After 2 months, allowing expression of the EYFP within the entirety of the transduced neurons
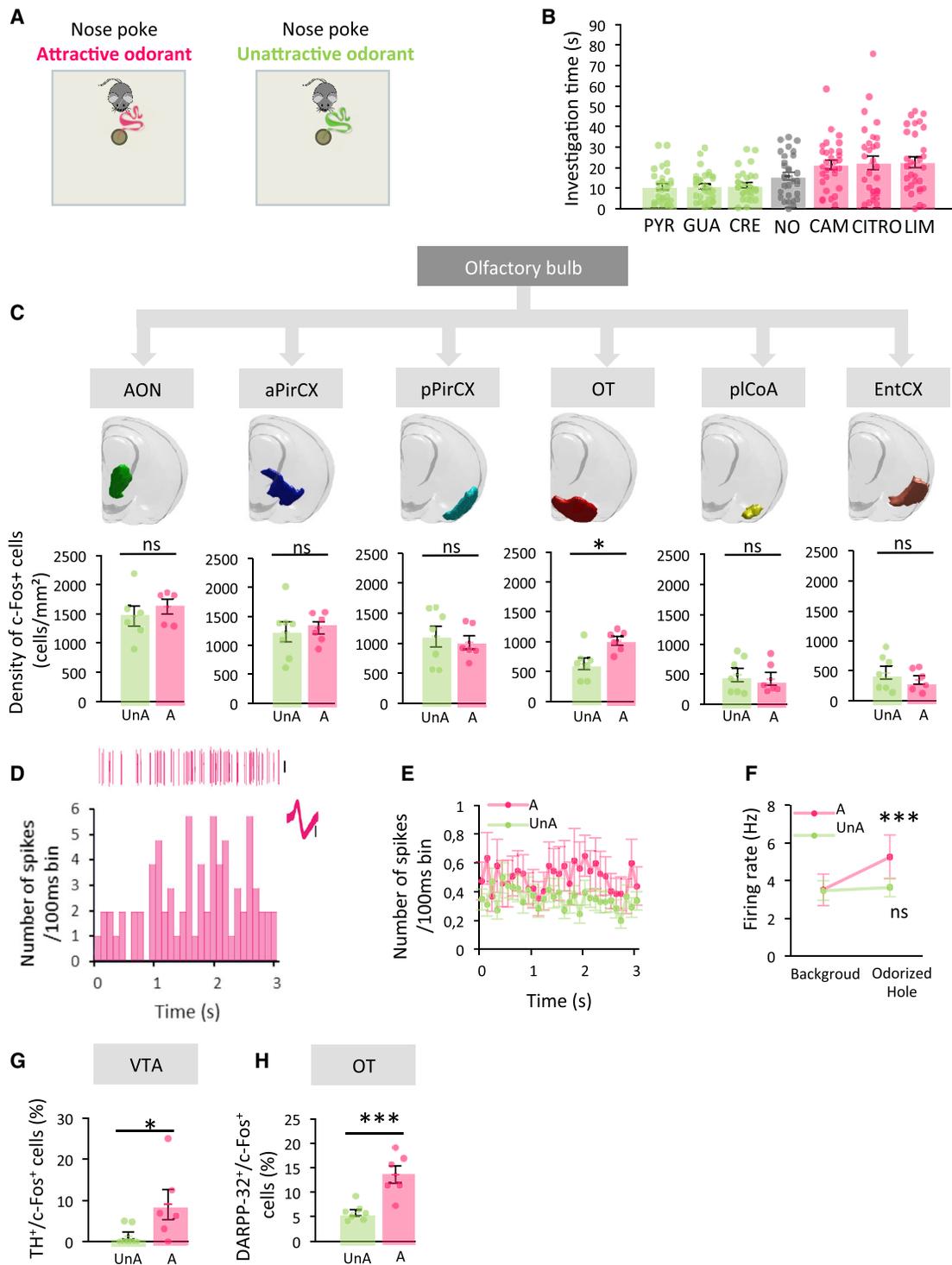
Figure 3. The OT, specifically, shows greater neural activity in response to attractive compared to unattractive odorants

(A) Experimental setup.

(B) Level of attraction of unlearned odorants (n = 30, green: unattractive odorant (UnA), gray: no odor (NO), pink: attractive odorant [A]). The level of attraction varied among odorants (Friedman Odor effect, $F_{(6,210)}$ = 27.86 p < 0.001, permutation test p < 0.001). Bars represent means of individual data points ± SEM.

(C) Top. ROI of secondary olfactory structures. Bottom. c-Fos+ cell density in response to UnA (n = 7) versus A (n = 6) odorants. No difference except in the OT (Bonferroni corrected One-Tailed Unpaired t-test, AON t = −0.704 p = 1 Cohen's d = −0.426, aPirCX t = −0.330 p = 1 Cohen's d = −0.184, pPirCX t = 0.477 p = 1 Cohen's d = 0.265, OT t = −2.991 p = 0.037 Cohen's d = −1.664, plCoA t = 0.380 p = 1 Cohen's d = 0.211, EntCX t = 0.860 p = 1 Cohen's d = 0.478). Bars represent means of individual data points ± SEM.

Current Biology
Article

CellPress

including their projecting axons,[6] EYFP was visualized using iDISCO.[18] The injection site was reconstructed with Imaris software[18] to validate the spread of the OB viral infection. In the brains showing localized injections either in the aOB or pOB, we observed that viral injections in the pOB (Figure 2A) led to a higher density of labeled fibers within the OT than viral injections in the aOB (Figure 2B).

To allow precise quantification of EYFP labeling, we performed additional groups of mice (aOB, n = 5; pOB, n = 5; Figure 2Ci) and confirmed a higher percentage of EYFP labeling in the OT's ventral surface (known to receive input from the OB) of mice injected in the pOB compared to mice injected in the aOB (EYFP labeling pOB = 0.155 ± 0.059%, aOB = 0.030 ± 0.010%; Bonferroni corrected One-Tailed Mann-Whitney, W = 2.000 p = 0.048 Rank-Biserial Correlation = −0.840; Figure 2Cii). Differences in the injection sites cannot account for this finding, since a similar percentage of transduced EYFP+ mitral cells (Tbx21+ neurons) was assessed in the OB of mice injected in the aOB or the pOB (Figure S2A-B).

In contrast to OT innervation, quantification of OB projections into the anterior (aPirCX) and posterior piriform cortex (pPirCX) revealed no difference of labeling based on the anterior or posterior OB injection sites (EYFP labeling in aPirCX pOB = 0.081 ± 0.039%, aOB = 0.105 ± 0.035%; EYFP labeling in pPirCX pOB = 0.078 ± 0.033%, aOB = 0.052 ± 0.019%; Bonferroni corrected One-Tailed Mann-Whitney, aPirCX W = 14.000 p = 1 Rank-Biserial Correlation = 0.120, pPirCX W = 11.000 p = 1 Rank-Biserial Correlation = −0.120; Figure 2Ciii and Civ). Altogether, these results highlight the existence of a privileged connection between the pOB and the OT that could support odorant attraction.

The olfactory tubercle, a key structure mediating odorant attraction

To now investigate the functional role of the OT in spontaneous attraction toward unlearned odorants, we used the one hole-board apparatus (Figure 3A) to quantify the duration of odor investigation as a measure for odor-driven attraction (Table S1).[6,19–21] In line with previous work, different odorants, chosen to be unfamiliar and with no particular biological significance (pyridine: PYR, guaiacol: GUA, p-cresol: CRE, control no odor: NO, camphor: CAM, citronellol: CITRO, +limonene: LIM) elicited diverse investigation times (Friedman test: Odor effect, $F_{(6,210)}$ = 27.86 p < 0.001, permutation test p < 0.001; Figure 3B).[6] Following behavioral testing, we used c-Fos labeling to map neural activity in response to the spontaneously investigated odorants. C-Fos+ cells were automatically detected on serial sections

of the anterior brain, and precisely allocated to specific brain regions, i.e., the direct synaptic targets of the OB (anterior olfactory nucleus: AON, aPirCX, pPirCX, OT, postero-lateral amygdala: plCoA and entorhinal cortex: EntCX) (Figure 3C; Figure S3A and Table S2).[22]

To uncover the spatial representation of activity underlying the attraction toward odorants independently of their identity, we averaged the activity evoked by each of the three spontaneously attractive (Attractive group, A) and the three spontaneously unattractive odorants (Unattractive group, UnA) used in the experiment (investigation time A = 22.040 ± 1.929 s, UnA = 10.950 ± 0.912 s; Two-Tailed Wilcoxon, W = 35.000 p < 0.001 Rank-Biserial Correlation = −0.849). Remarkably, we found no difference of c-Fos+ cell density in any of the secondary olfactory areas between odorant groups except for the OT (c-Fos+ cell in OT A = 1014.090 ± 73.140 cells/mm^2, UnA = 631.194 ± 100.211 cells/mm^2; Bonferroni corrected One-Tailed Unpaired t-test, AON t = −0.704 p = 1 Cohen's d = −0.426, aPirCX t = −0.330 p = 1 Cohen's d = −0.184, pPirCX t = 0.477 p = 1 Cohen's d = 0.265, OT t = −2.991 p = 0.037 Cohen's d = −1.664, plCoA t = 0.380 p = 1 Cohen's d = 0.211, EntCX t = 0.860 p = 1 Cohen's d = 0.478; Figure 3C). Indeed, the OT showed a higher density of c-Fos+ cell density in response to attractive compared to unattractive odorants (Figure 3C). This difference arose principally from its medial domain (mOT) compared to the lateral OT (lOT) (Figure S3C).

To confirm that the increase of c-Fos expression observed in the OT reflects an increase in neural activity during odor sampling itself, we directly probed the activity of the mOT in freely moving mice, using an eight-channel electrode array implanted in the mOT (Figure S3D). Extracellular single-unit recordings of mOT activity were performed during 120 s trials in which mice were allowed to explore the hole-board. Each mouse was tested in different trials with the three attractive (LIM, CITRO, CAM) and the three unattractive odorants (PYR, CRE, GUA). We first confirmed that the distribution of attraction to odorants is similar to that shown on Figure 3B (Kolmogorov-Smirnov p = 0.100), thus replicating the previous behavioral data. Although attractive and unattractive odorants led to similar firing rate throughout the entire 120 s of the trial (background firing rate A = 3.512 ± 0.846Hz, UnA = 3.456 ± 0.512Hz; One-Tailed Mann-Whitney W = 2610.000 p = 0.237 Rank-Biserial Correlation = −0.070), approach (defined by the 3 s phase preceding the nose poke) toward attractive odorants resulted in a significant increase in firing frequency compared to background firing (firing rate for A Odorized Hole = 5.248 ± 1.155Hz, firing rate for UnA Odorized Hole = 3.637 ± 0.496Hz; Bonferroni corrected One-Tailed Wilcoxon for

(D) Activity of a single OT neuron during the 3 s period preceding the first hole investigation in response to the A odorant CITRO. Data include example spike events (top), firing histogram (bottom) and overdrawn waveform (inset). Scale bars represent 0.1mV.

(E) Population average values for all recorded neurons in the OT during the 3 s period preceding the first hole investigation by mice (n = 10) in response to A (n = 55 units) or UnA odorants (n = 102 units). Values represent means ± SEM.

(F) Firing rate across the entire trial (background) and during the 3 s period preceding the first hole investigation (Odorized Hole). Firing rate increased when animals (n = 10) approached A (n = 55 units) but not UnA odorants (n = 102 units) compared to background (Bonferroni corrected One-Tailed Wilcoxon, A W = 354.000 p < 0.001 Rank-Biserial Correlation = −0.523, UnA W = 2185.000 p = 0.136 Rank-Biserial Correlation = −0.168). Values represent means ± SEM. (G) A higher percentage of TH+ cells expressing c-Fos in the VTA is observed in A (n = 6) compared to UnA group (n = 5) (One-Tailed Unpaired t-test, t = −2.176 p = 0.026 Cohen's d = −1.211). Bars represent means of individual data points ± SEM.

(H) A higher percentage of DARPP-32+ cells expressing c-Fos in the OT is observed in A (n = 6) compared to UnA group (n = 5) (One-Tailed Unpaired t-test, t = −4.369 p = < 0.001 Cohen's d = −2.431). Bars represent means of individual data points ± SEM *p < 0.05, ***p < 0.001.
See also Tables S1, S2, and Figure S3.
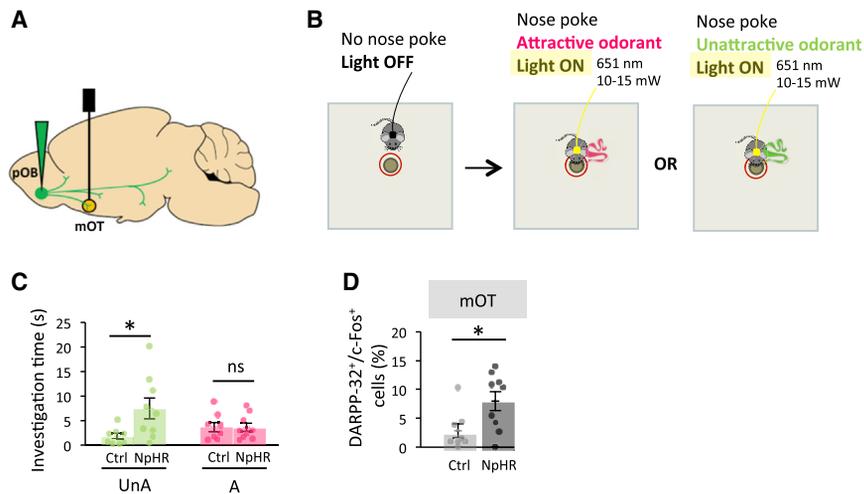
Figure 4. Impact of pOB-mOT pathway activity on odor-driven attraction

(A) Injection of NpHR-EYFP (NpHR; n = 9) or control virus (Ctrl; n = 8) in the mitral cells layer of the pOB and optical fiber implantation in mOT.

(B) The bilateral continuous light stimulation was automatically triggered by mice nose poking within 1 cm zone around the odorized hole (attractive or unattractive odorants) and stopped automatically when nose poke stopped.

(C) Inhibition of pOB-mOT pathway activity increased mice attraction toward unattractive odorants (UnA; Bonferroni corrected Two-Tailed Mann-Whitney, W = 12.000 p = 0.047 Rank-Bise-rial Correlation = −0.667) but not toward attractive ones (A; Bonferroni corrected Two-Tailed Mann-Whitney, W = 36.000 p = 1 Rank-Biserial Correlation = 0.000). Bars represent means of individual data points ± SEM.

(D) The percentage of DARPP-32+ cells expressing c-Fos was higher in NpHR mice compared to Ctrl in mOT (Bonferroni corrected One-Tailed Mann-Whitney, W = 13.500 p = 0.034 Rank-Biserial Correlation = −0.625). Points represent individual data ± SEM *p < 0.05.

See also Table S1 and Figure S4.

comparison to background, A W = 354.000 p < 0.001 Rank-Bise-rial Correlation = −0.523, UnA W = 2185.000 p = 0.136 Rank-Bi-serial Correlation = −0.168; Figures 3D–3F). Thus, during this time window, the mOT activity is modulated by the hedonic value of the odorant and the animal can use the odor cue emanating from the hole to initiate its approach to the odor source. These results support that the mOT encodes attraction to odorants.

To further explore the link between OT activation during attraction to odor and the triggering of the motivated behavior, we next studied the recruitment of the OT-VTA network. We assessed activity of VTA dopaminergic neurons ($TH^+/c\text{-}Fos^+$) and OT medium spiny neurons ($DARPP\text{-}32^+/c\text{-}Fos^+$) in response to odorants. We found a higher percentage of double-labeled cells in both structures in response to attractive versus unattractive odorants ($TH^+/c\text{-}Fos^+$ cells A = 8.962 ± 3.632% UnA = 1.395 ± 0.901%, $DARPP\text{-}32^+/c\text{-}Fos^+$ cells A = 13.604 ± 1.779% UnA = 5.830 ± 0.647%; One-Tailed Unpaired t-test, VTA t = −2.176 p = 0.026 Cohen's d = −1.211, OT t = −4.369 p < 0.001 Cohen's d = −2.431; Figures 3G and 3H). Altogether, these data highlight a key role of the OT in encoding odor-driven attraction.

### The pathway between the posterior olfactory bulb and the medial olfactory tubercle drives odorant attraction

To uncover the functional involvement of the pOB-mOT pathway in driving odorant attraction, we modulated pOB-mOT activity during mice approach toward odorants. Two groups of mice were injected with a Lenti-hSyn-eNpHR3.0-EYFP virus (NpHR group) or a control Lenti-hSyn-EYFP virus (Ctrl group) in the ventro-posterior mitral cell layer of the OB with optical fibers implanted in mOT (Figure 4A; Figures S4A and S4B). Mice were placed on the odorized hole board and bilateral light stimulation was automatically triggered when mice nose poked within 1 cm around the hole (light-triggering zone) and lasted as long as the nose poke (Figure 4B). The hole contained attractive or unattractive odorants and each mouse was tested in the two conditions. First, Ctrl mice spent more time investigating attractive odorants than unattractive ones (investigation time A = 3.683 ± 0.962 s UnA = 1.793 ± 0.602 s; One-Tailed Wilcoxon W = 31.000 p =

0.034 Rank-Biserial Correlation = 0.722), indicating no effect of light per se on odor-driven attraction. We then found that optogenetic inhibition of the pOB-mOT path increased investigation time of unattractive odorants (NpHR = 7.451 ± 2.135 s versus Ctrl = 1.793 ± 0.602 s; Bonferroni corrected Two-Tailed Mann-Whitney, W = 12.000 p = 0.047 Rank-Biserial Correlation = −0.667). The investigation time of attractive odorants was not different between NpHR and Ctrl mice (NpHR = 3.600 ± 0.849 s; Ctrl = 3.683 ± 0.962 s; Bonferroni corrected Two-Tailed Mann-Whitney, W = 36.000 p = 1 Rank-Biserial Correlation = 0.000; Figure 4C).

We then assessed the effect of the optogenetic manipulation on mOT neuronal activity and found a higher percentage of medium spiny neurons expressing c-Fos ($DARPP\text{-}32^+/c\text{-}Fos^+$) in NpHR than in Ctrl mice ($DARPP\text{-}32^+/c\text{-}Fos^+$ cells, NpHR = 7.969 ± 1.652% EYFP = 2.863 ± 1.192%; Bonferroni corrected One-Tailed Mann-Whitney, W = 13.500 p = 0.002 Rank-Biserial Correlation = −0.625; Figure 4D). No effect of optogenetic manipulation on neuronal activity was observed in lOT confirming the main effect of optogenetic stimulation in the mOT (Figure S4C). Altogether, these results demonstrated that the pOB modulated activity of mOT and enabled increasing attraction to unpleasant odorants.

Attractive odorants induce conditioned place preference mediated by dopamine signaling

A classic way of testing the functional recruitment of the reward system by a given stimulus is to investigate whether this stimulus is able to serve as a reinforcer.[23–25] Conditioned place preference (CPP) is a well-established test to measure the reinforcing effects of a stimulus by evaluating if animals develop a preference for the location where they received the stimulus. To further confirm the rewarding property of attractive odorants, we assessed whether mice can be conditioned in an odorant place preference paradigm. Following a period of habituation, we conditioned mice by alternatively confining them in two distinct compartments, one of which contained the odorant of interest (4 sessions of 15 min/day across 5 days) (Figure 5A) and the other compartment contained no odorant. Before (pre-conditioning) and after (post-conditioning) the conditioning phase, mice were allowed to freely

Current Biology
Article

CellPress
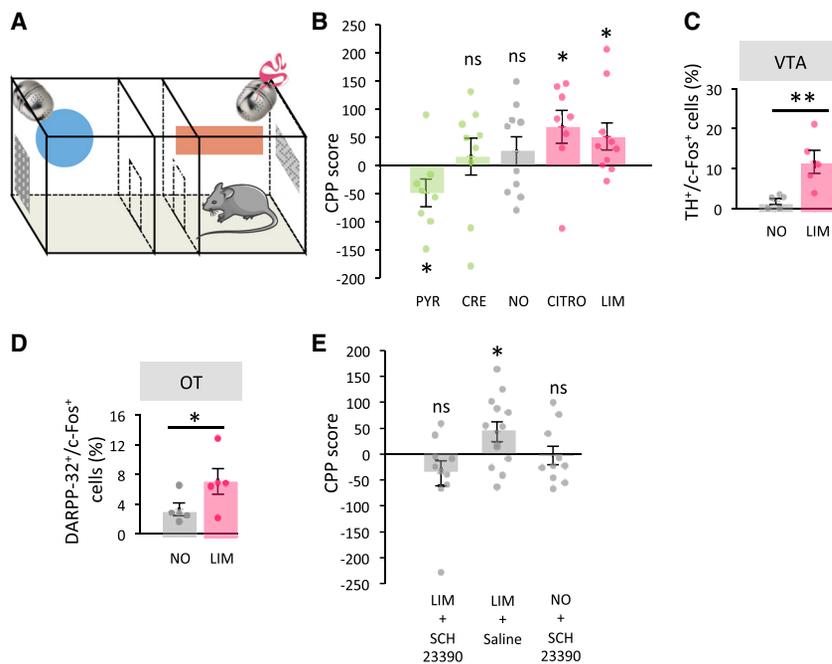
Figure 5. Spontaneously attractive odorants induce conditioned place preference

(A) Schema of conditioned place preference (CPP) apparatus.

(B) CPP score (time in s spent in the odor paired compartment during post-conditioning – pre-conditioning test) is different between experimental groups. Only attractive odorants (CITRO n = 8, LIM n = 10) induced CPP (One-Tailed One-Sample t-test, CITRO t = 2.331 p = 0.026 Cohen's d = 0.824, LIM t = 2.123 p = 0.031 Cohen's d = 0.671). Unattractive ones (CRE n = 9, PYR n = 8) induced no CPP (One-Tailed One-Sample t-test, CRE t = 0.473 p = 0.324, Cohen's d = 0.158) or aversion (One-Tailed One-Sample t-test, PYR t = −1.974 p = 0.045, Cohen's d = −0.698). Control group (NO, n = 10) showed no CPP (One-Tailed One-Sample t-test, NO t = 1.005 p = 0.171 Cohen's d = 0.318). Bars represent means of individual data points ± SEM.

(C) The percentage of TH+ cells expressing c-Fos in VTA was higher in mice conditioned with LIM (n = 5) compared to NO mice (n = 5) (One-Tailed Unpaired t-test, t = −3.302 p = 0.005, Cohen's d = −2.088). Bars represent means of individual data points ± SEM.

(D) The percentage of DARPP-32+ cells expressing c-Fos in OT was higher in LIM conditioned (n = 5) compared to control (n = 5) mice (One-Tailed Unpaired t-test, t = −1.968 p = 0.042, Cohen's d = −1.245). Bars represent means of individual data points ± SEM.

(E) CPP to LIM was suppressed by D1 receptor antagonist SCH23390 (LIM+SCH23390, n = 10) (Two-Tailed One-Sample t-test, t = −1.509 p = 0.166, Cohen's d = −0.477). This was not observed after Saline infusion (LIM+Saline, n = 13) (Two-Tailed One-Sample t-test, t = 2.258 p = 0.043, Cohen's d = 0.626) and no conditioned aversion was observed in control group injected with SCH23390 (NO+SCH23390, n = 10) (Two-Tailed One-Sample t-test, t = −0.180 p = 0.861, Cohen's d = −0.057) indicating that drug alone did not induce avoidance. Bars represent means of individual data points ± SEM *p < 0.05, **p < 0.01.
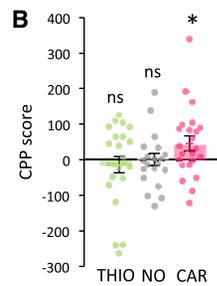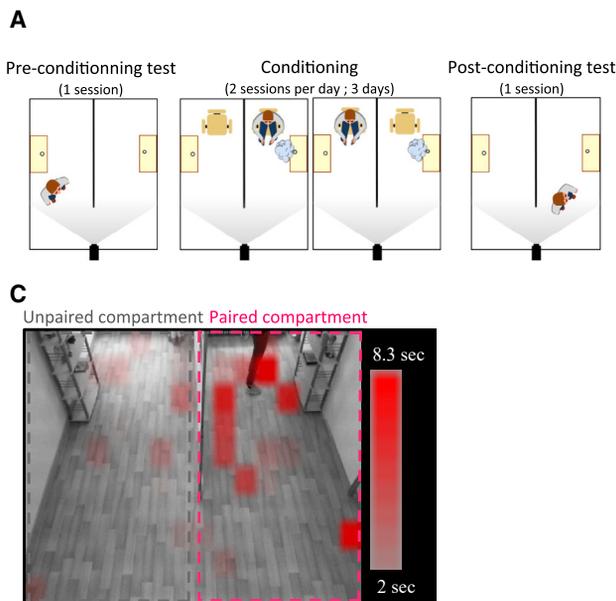
See also Table S1 and Figure S5.

explore both compartments in the absence of reinforcer (odorant), and the time spent in each of them was recorded. Changes in the time spent in the stimulus-paired compartment between pre-conditioning and post-conditioning is calculated as an index of the preference for the reinforced compartment (conditioned place preference score) and thus of the reinforcing effect of the stimulus.[24] In a first series of experiments, five groups of mice were tested, two groups were trained with spontaneously attractive odorants (CITRO or LIM, n = 8 and 10, respectively), two with spontaneously unattractive odorants (PYR or CRE, n = 8 and 9, respectively), and a control group of mice was submitted to the same sequence of behavior but in the absence of odorant (NO, n = 10) (Table S1).

We found that mice spent more time in the compartment previously paired with a spontaneously attractive odorant indicating a place preference conditioning induced by attractive odorant and thus a rewarding effect of the odorants (CPP score CITRO = 68.705 ± 29.480 s LIM = 50.869 ± 23.963 s; One-Tailed One-Sample t-test, CITRO t = 2.331 p = 0.026 Cohen's d = 0.824 LIM t = 2.123 p = 0.031 Cohen's d = 0.671; Figure 5B). Second, mice spent less time in the compartment previously paired with one of the two unattractive odorants (PYR) (CPP score PYR = −48.900 ± 24.000 s; One-Tailed One-Sample t-test, t = −1.974 p = 0.045 Cohen's d = −0.698; Figure 5B) indicative of a conditioned place aversion. CRE group and control animals (NO) showed neither place preference nor aversion (CPP score CRE = 15.678 ± 33.127 s NO = 25.405 ± 25.271 s; One-Tailed One-Sample t-test, CRE t = 0.473 p = 0.324 Cohen's d = 0.158 NO t = 1.005 p = 0.171 Cohen's d = 0.318; Figure 5B). These

results showed that attractive odorants possess positive reinforcing properties. Further, these results demonstrated that at least one unattractive odorant can have an opposite effect and induce a conditioned place aversion showing negative reinforcing properties.

To go further, we analyzed the neural activity within both the OT and the VTA using assessment of c-Fos expression, in medium spiny neurons (DARPP-32+ cells) and dopaminergic cells (TH+ cells), respectively, following place preference in response to an odorant (LIM-CPP versus control NO groups). We found a higher percentage of double-labeled cells in both neuronal populations in LIM-CPP compared to control NO group (TH+/c-Fos+ cells LIM = 11.726 ± 2.894% NO = 1.841 ± 0.764%, DARPP-32+/c-Fos+ cells LIM = 7.055 ± 1.706% NO = 3.301 ± 0.853%; One-Tailed Unpaired t-test, t = −3.302 VTA p = 0.005 Cohen's d = −2.088 and OT t = −1.968 p = 0.042 Cohen's d = −1.245; Figures 5C and 5D), indicating an activation of both OT and VTA by CPP.

Since the release of dopamine (DA) within the reward system is a common substrate of rewarding stimuli,[12] we performed a second series of experiments aimed at altering dopaminergic transmission during odor CPP to more directly assess the recruitment of the reward system by spontaneously attractive odorants. In a first group of animals, the DAergic D1 receptor antagonist SCH23390[26,27] was systemically injected 15 min before confinement in the LIM-paired compartment while saline was injected 15 min before confinement in the unpaired compartment (LIM+SCH23390 group). Remarkably, D1 antagonism suppressed LIM-induced CPP in the LIM+SCH23390 group while mice of

A

Pre-conditionning test
(1 session)

Conditioning
(2 sessions per day ; 3 days)

Post-conditioning test
(1 session)

B

C

Unpaired compartment Paired compartment

8.3 sec

2 sec

Figure 6. Attractive odorant induced conditioned place preference in humans
(A) Schema of conditioned place preference paradigm (CPP).
(B) CPP score in odor paired compartment was calculated as follows, time spent in the conditioned compartment during post-conditioning – pre-conditioning. CAR (n = 23) (One-Tailed One-sample t-test, t = 2.219 p = 0.019, Cohen's d = 0.463) and not control (NO, n = 21) (One-Tailed One-sample t-test, t = 0.043 p = 0.483, Cohen's d = 0.009) or THIO (n = 23) (One-Tailed One-sample t-test, t = −0.592 p = 0.280, Cohen's d = −0.123) induce CPP. Bars represent means of individual data points ± SEM.
(C). CAR-CPP score representation in discretized space of CPP apparatus. *p < 0.05.
See also Table S1 and Figure S6.

second group injected with saline (LIM+Saline group) continued expressing CPP (CPP score LIM+SCH23390 = −37.033 ± 24.547 s LIM+Saline = 42.705 ± 18.916 s; Two-Tailed One-Sample t-test, LIM+SCH23390 t = −1.509 p = 0.166 Cohen's d = −0.477, LIM+Saline t = 2.258 p = 0.043 Cohen's d = 0.626; Figure 5E), similarly to non-injected mice (Figure 5B). Importantly, because the OB contains DAergic periglomerular interneurons involved in odor processing, we verified that SCH23390 did not alter LIM detection (Figure S5A). In addition, to exclude any adverse effect of SCH23390, we performed testing in an additional control group in which SCH23390 injection was paired to one of the two compartments without any odorant (NO+-SCH23390 group) to confirm that the drug alone did not induce conditioned place aversion (CPP score NO+SCH23390 = −3.210 ± 17.833 s; Two-Tailed One-Sample t-test, NO+-SCH23390 t = −0.180 p = 0.861 Cohen's d = −0.057; Figure 5E). Notably, we observed a reduction in the average locomotion speed of mice during confinement (Figure S5B) following SCH23390, in line with alteration of locomotion associated with dopaminergic antagonists.[28] However, because SCH23390 was injected during the conditioning phase only (confinement) and not during pre-conditioning or post-conditioning tests, and since a 24 h wash-out was allowed between SCH23390 injection and testing, we reason that the speed reduction is not a major influencer on the CPP score. Together, these results show that dopamine signaling bestows odorants with rewarding properties thereby driving their spontaneous attraction.

Attractive odorants induce conditioned place preference in humans

To analyze whether our observations can be extended to humans, 67 participants (34 women, 35 men) between the ages of 18 and 30 years (mean ± SD, 21.5 ± 2.6 years) were recruited to take part in a similar CPP test. The CPP that is classically used in the animal model to evaluate the rewarding power of a stimulus (such as drugs or food), has also occasionally been applied to humans.[29,30] In our study, the CPP facility consisted of an experimental room separated into two compartments of the same size, shape, and furnishing but clearly distinguishable based on decorative elements (Figure 6A). As in mice, before and after a conditioning phase (2 sessions of 10 min/day across 3 days) in which participants were alternatively confined in two distinct compartments, one of which contained an attractive odorant (L-carvone: CAR; n = 23) and the other one no odorant, participants were allowed to freely explore both compartments in the absence of odorant and the time spent in each of them was compared between pre- and post-conditioning test. The odorant CAR was selected since this odorant is rated as strongly attractive in humans.[20,31,32] When comparing the time spent in each compartment in the post-conditioning versus the pre-conditioning phases, we found that participants spent more time in the room previously paired with CAR (CPP score CAR = 45.877 ± 20.678 s; One-Tailed One-sample t-test t = 2.219 p = 0.019 Cohen's d = 0.463; Figures 6B and 6C), indicating an odor–driven CPP in humans.

To validate this result, two additional experimental groups were tested. First, a control no odor group (NO; n = 21) was found to display no place preference following being subjected to the same behavioral paradigm but with no odor associated to any compartment (CPP score NO = 0.738 ± 17.091 s; One-Tailed One-sample t-test t = 0.043 p = 0.483 Cohen's d = 0.009; Figure 6B). Second, we also tested the effect of CPP training with an unattractive odorant (thioglycolic acid: THIO; n = 23) and found no place preference (CPP score THIO = −13.801 ± 23.330 s; One-Tailed One-sample t-test t = −0.592 p = 0.280 Cohen's d = −0.123; Figure 6B). We verified that the CPP scores cannot be explained by a spontaneous preference for one specific compartment (Figure S6A) or by a difference in intensity perception between the two odorants (Figure S6B). We also confirmed that odorant smelled during the conditioning phase by the CAR group was rated as more attractive than by the THIO group (Figure S6C). Taken together, these results show that spontaneously attractive odorants are rewarding in humans as they are in mice when assessed by CPP.

Current Biology
Article

 CellPress

The activity of the olfactory tubercle reflects the odorants attraction in humans

We finally confirmed the recruitment of the human OT by attractive odorants. 30 volunteers were asked to rate, during an fMRI session, the attraction of seven odorants (butanoic acid: BUT, 3-hydroxy-3-methylhexanoic acid: HMHA, 3-methyl-3-sulfanylhexan-1-ol: MSH, cis-3-hexenol: CIS3, terpinen-4-ol: TER, +limonene: LIM and isoamyl acetate: ISO) from 1 (weakly/unattractive) to 5 (highly attractive) during a fMRI recording session (Table S1). For each participant, odorants rated from 3 to 5 were classified in the "attractive group," whereas odorants rated 1 or 2 were classified in the "unattractive group." First, as expected, we found activation in olfactory areas including the PirCX and area bordering the OT in response to odorants (Figure 7A). Sniffing was digitally recorded during the experiment and was used as a covariate in the fMRI contrast estimation. The fMRI images were then averaged within the two attraction conditions based on the individual odorant rating (attractive ratings, unattractive ratings). Then, mean activity levels were measured in the OT, aPirCX, and pPirCX using ROIs. Mean activity of the OT, aPirCX, and pPirCX were averaged between hemispheres (no hemisphere*attraction interaction, Repeated-measure ANOVA, OT $F_{(3,120)} = 0.12$ p = 0.914, aPirCX $F_{(3,120)} = 0.94$ p = 0.336, pPirCX $F_{(3,120)} = 0.07$ p = 0.797). These results uncovered higher OT activation in response to the attractive odorants compared to those unattractive (Mean βvalue A = 2.109 ± 0.821 UnA = 0.708 ± 0.706; Bonferroni corrected One-Tailed Paired t-test, OT t = 2.572 p = 0.023 Cohen's d = 0.470; Figures 7B–7D), whereas no difference was found in either the aPirCX or pPirCX (Mean βvalue in aPirCX A = 2.342 ± 0.609 UnA = 1.823 ± 0.507, Mean βvalue in pPirCX A = 3.148 ± 0.799 UnA = 2.515 ± 0.738; Bonferroni corrected One-Tailed Paired t-test, aPirCX t = 1.320 p = 0.296 Cohen's d = 0.241, pPirCX t = 1.081 p = 0.432 Cohen's d = 0.197; Figures 7E–7J). This confirms the selective recruitment of the OT by attractive odorants.

DISCUSSION

Our close relationship with smells exemplifies the strong attractive power they exert over us. Why do some odorants possess such strong effects? This study provides behavioral, anatomical, and functional evidence that odorants can act as natural rewards in the absence of associated food or social cues.

We first discovered that the pOB supports self-stimulation conditioning, suggesting that this sensory structure strongly interfaces with the reward system. Multiple brain areas support self-stimulation operant conditioning, especially those in the reward system.[10,11] These areas include the VTA itself, as well as its direct synaptic targets such as the nucleus accumbens, the prefrontal cortex, or the septum. Self-stimulation conditioning can also be obtained from brain areas projecting to the VTA such as the OT or the hypothalamus.[33,34] Our data reveal that the pOB, not receiving from nor sending direct synaptic contacts to the VTA, supports self-stimulation conditioning, in line with an isolated report from the early 1970s suggesting electrical self-stimulation in the rat OB.[35] Thus, our results highlight an unexpectedly new region-dependent role of the OB, and therefore the rewarding power of odorants. We found that attractive odorants induced DA-

dependent CPP, indicating that they have reinforcing properties as other well-known natural reinforcers, such as food or mating.[36,37] Importantly, we were able to show that pleasant odorants can drive CPP in humans, suggesting that the reinforcing properties of odorants are not limited to macrosmic animals but perpetuate in humans. Further, our finding that the pOB but not the aOB is a site for self-stimulation has two major implications. First, this strongly suggests that hedonic representations of odorants are incentive information relayed to the reward system to induce attraction. Second, it confirms that the olfactory system's representation of hedonics is functionally partitioned along its antero-posterior axis.[6] Consistent with a dual processing of olfactory hedonics, we also found that at least some unattractive odorants can induce conditioned place aversion.

The next question we addressed relates to the brain circuit accounting for the behavioral reinforcing properties of odorants. pOB self-stimulation activated the DAergic neurons of the VTA and the relay neurons of the OT indicating actual recruitment of the reward system that could form the neural basis of the incentive value of attractive odorants. Furthermore, both unit recordings and c-Fos cell mapping indicated that the OT responded selectively to the exposure of attractive odorants. Remarkably, c-Fos cell mapping data further revealed that among all the direct synaptic targets of the OB, only the OT exhibits a selective response with regard to odor hedonic tone. Consistently, increasing MSNs activity through optogenetic manipulation of the pOB-mOT pathway made unattractive odorant more attractive. This effect was obtained by local optogenetic inhibition of mitral cells which project to the GABAergic interneurons of the OT layer1, possibly leading to MSNs disinhibition.[38]

It is tempting to relate the hedonic-specific responses of the OT to its location at the cross road between the olfactory and reward systems and more specifically the VTA to which the OT is connected.[12,13,38] In animal models, the role of the OT in processing attractive or aversive odorants with strong ethological significance such as food, predator or opposite-sex odors[15,39] or learned odorants that predict a reward[13,16,17,40] is well documented. Here, we provide evidence for a new role of the OT– that being in processing attraction induced by unlearned odorants. Moreover, the direct stimulation of OT[39] or the modulation of the VTA-mOT pathway[40] are known to modify olfactory preferences; here, we revealed that afferent projections from pOB to mOT are also implicated in the build-up of odor-driven attraction.

We rigorously identified that the pOB sends denser projections to the OT than the aOB does. This distinct pattern of connectivity from the aOB or the pOB to the OT may relate to the timing of mitral cell development[41] and adds a layer to the functional significance of the distribution of hedonic information along the antero-posterior axis of the OB. Finally, the privileged connection between the pOB and the OT highlighted the pOB-OT-VTA axis as a key pathway for processing odor information and converting it into motivated behavior. A question of interest for future investigation relates to how the activity of such hard-wired pathway is modified or overcome as the initial odorant value is changed by learning or experience.

The role of the OT in coding odor hedonics in humans remained controversial.[42,43] Using ROI analysis to take into account the anatomical variabilities between subjects, our findings bring new evidence for selective activation of the OT, but
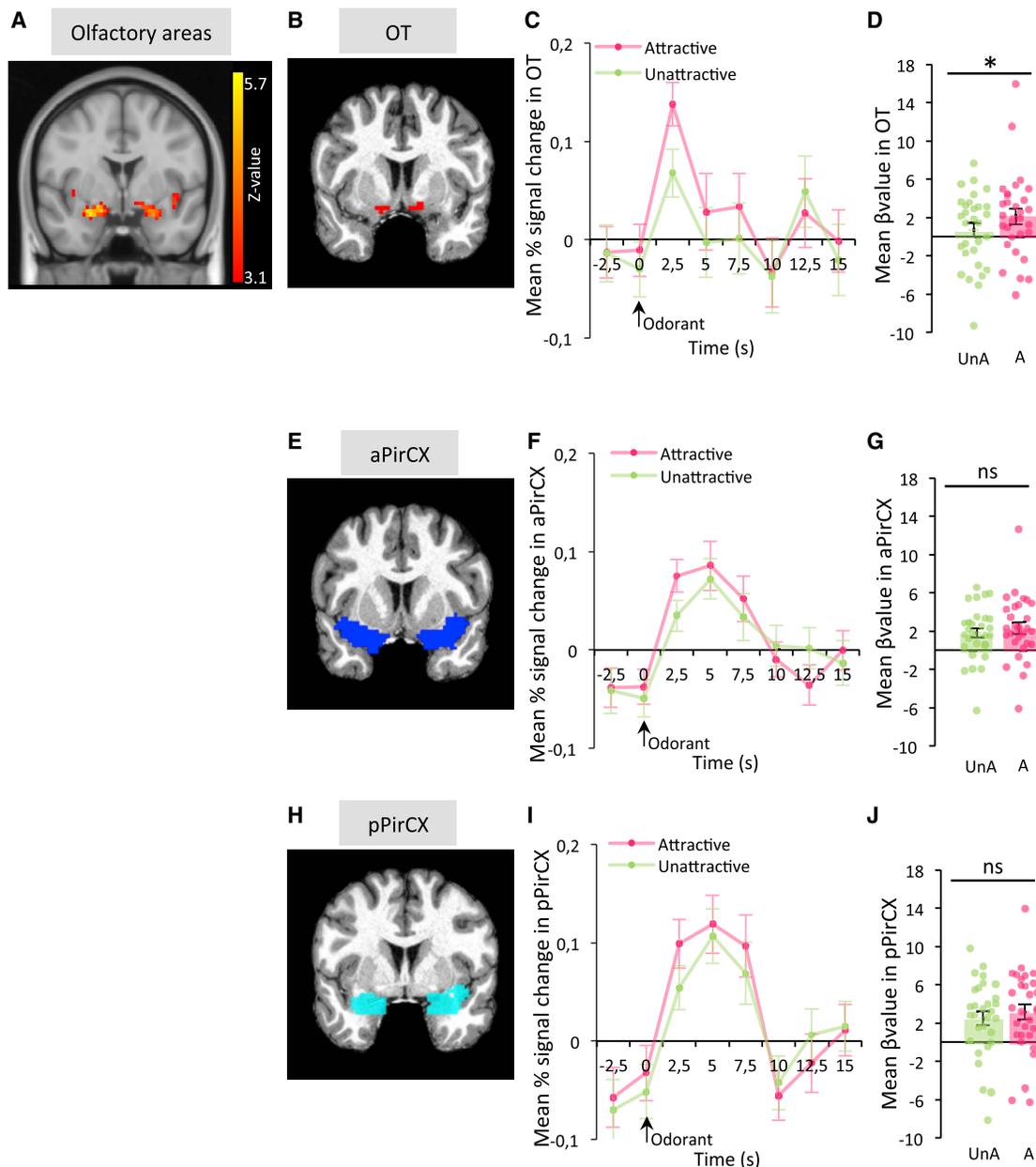
Figure 7. Attractive odorants specifically activate the OT in humans
(A) Brain activity in response to odorants (n = 30 subjects). Brain activity was present in the olfactory areas including the PirCX and bordering the OT.
(B) Example of OT ROI for one participant.
(C) OT activity in response to attractive (A) or unattractive (UnA) odorants. Values represent means ± SEM.
(D) The OT showed higher level of activity in response to A compared to UnA odorants (Bonferroni corrected One-Tailed Paired t-test, t = 2.572 p = 0.023, Cohen's d = 0.470). Bars represent means of individual data points ± SEM.
(E) Example of aPirCX ROI for one participant.
(F) aPirCX activity in response to A or UnA odorants. Values represent means ± SEM.
(G) There is no difference of activity in the aPirCX between A and UnA odorants (Bonferroni corrected One-Tailed Paired t-test, t = 1.320 p = 0.296, Cohen's d = 0.241). Bars represent means of individual data points ± SEM.
(H) Example of pPirCX ROI for one participant.
(I) pPirCX activity in response to A or UnA odorants. Values represent means ± SEM J. The activity in pPirCX was similar between response to A and UnA odorants (Bonferroni corrected One-Tailed Paired t-test, t = 1.081 p = 0.432, Cohen's d = 0.197). Bars represent means of individual data points ± SEM *p < 0.05.
See also Table S1.

Current Biology
Article

🔒 CellPress

not of the PirCX, in response to attractive odorants. Thus, our data obtained in mice were confirmed in humans, suggesting a highly conserved role of the OT between mice and humans, despite anatomical differences between the two species. In rodents, the OT is visible as a round bulge that covers a wide area of the basal forebrain and is located between the lateral olfactory tract and the optic chiasm.[13] Data from human brain imaging identified it as a small structure ventrally located to the anterior olfactory cortex, between the uncus and the medial forebrain bundles.[44,45] Despite these regional differences, the OT is targeted by the OB output, making it a structure belonging to the primary olfactory cortex both in humans[46] and rodents.[13] Interestingly, the PirCX showed no change in activity according to odor hedonics. The PirCX contributes to odor identity coding, habituation mechanisms, olfactory learning, and memory.[47–54] Several studies carried out in humans and animals also argued in favor of the involvement of PirCX in the representation of odor hedonics.[53,55–61] This apparent discrepancy with our data may arise from the use of odorants in a learning context or with strong biological meaning. The odorant cerebral representation may thus reflect associative and hedonic characteristics related to smell. Indeed, the role of the PirCX in encoding associative olfactory information is well documented.[62–66] Finally, the different functional roles of the OT and PirCX can be explained by their difference of brain connectivity. fMRI whole-brain functional connectivity cluster analysis yields different clusters corresponding respectively to OT and PirCX,[46] making the OT a specific pathway for spontaneous odorant-driven attraction.

Altogether, these data demonstrate that unlearned attractive odorants are rewarding in mice and humans thanks to strong functional and anatomical connections between the OB and the OT thereby allowing a shortcut entrance of olfactory information in the reward system. Several stimuli are known to be rewarding in humans, including sweet tastes, money, smiling faces, some artwork, and some music.[67–70] Preferred music induces a release of dopamine in striatal regions[68] and administration of dopamine precursor or antagonist respectively enhanced or decreased music motivated responses.[69] It is worth noting that not all sensory stimuli are rewarding. For instance, only preferred music (and not random music) recruits the reward system.[68] In line with this, we found that not all odorants are rewarding, but only attractive ones. These data suggest that the involvement of the reward system is based on intrinsic hedonic properties of sensory stimuli and not a global rewarding effect of sensory arousal.[71]

In sum, our data propose a direct gateway from the olfactory bulb to the reward system as the neural basis of the strong and persistent attraction of some odors.

STAR★METHODS

Detailed methods are provided in the online version of this paper and include the following:

- KEY RESOURCES TABLE
- RESOURCES AVAILABILITY
  - ○ Lead contact
  - ○ Materials availability
  - ○ Data and code availability

- EXPERIMENTAL MODEL AND SUBJECT DETAILS
- METHOD DETAILS
  - ○ Cell analysis
  - ○ Optogenetic intracranial self-stimulation
  - ○ iDISCO
  - ○ Quantification of OB-OT neural projections
  - ○ c-Fos mapping of the olfactory secondary areas
  - ○ Olfactory tubercle in vivo electrophysiology
  - ○ pOB-mOT optogenetic inhibition
  - ○ Odor conditioned place preference
  - ○ D1 receptor blockade during CPP
  - ○ Conditioned place preference in humans
- QUANTIFICATION AND STATISTICAL ANALYSIS
  - ○ fMRI study
- EXPERIMENTAL PROCEDURE
  - ○ Preprocessing
  - ○ Statistical analysis
- QUANTIFICATION AND STATISTICAL ANALYSIS

AUTHOR CONTRIBUTIONS

M.M., L.C., N.R., M.T., N.N., C.F., A.F., D.W.W., M.B., A.D., and N.M., designed the experiments. M.M., L.C., N.R., A.M., M.T., J.S., M.B., J.F., C.F., A.F., and N.M. conducted the experiments. M.M., L.C., N.R., M.R., O.R., M.B., A.D., and N.M. wrote the paper.

DECLARATION OF INTERESTS

The authors declare no competing interests.

REFERENCES

1. Schiffman, S., Robinson, D.E., and Erickson, R.P. (1977). Multidimensional scaling of odorants: examination of psychological and physicochemical dimensions. Chem. Senses 2, 375–390.

2. Richardson, J.T., and Zucco, G.M. (1989). Cognition and olfaction: a review. Psychol. Bull. 105, 352–360.

3. Yeshurun, Y., and Sobel, N. (2010). An odor is not worth a thousand words: from multidimensional odors to unidimensional odor objects. Annu. Rev. Psychol. 61, 219–241.

4. Walliczek-Dworschak, U., and Hummel, T. (2017). The Human Sense of Olfaction. Facial Plast. Surg. 33, 396–404.

5. Kosaka, T., and Kosaka, K. (2009). Olfactory Bulb Anatomy. In Encyclopedia of Neuroscience, L.R. Squire, ed. (Academic Press), pp. 59–69.

6. Kermen, F., Midroit, M., Kuczewski, N., Forest, J., Thévenet, M., Sacquet, J., Benetollo, C., Richard, M., Didier, A., and Mandairon, N. (2016). Topographical representation of odor hedonics in the olfactory bulb. Nat. Neurosci. 19, 876–878.

7. Schultz, W. (1998). Predictive reward signal of dopamine neurons. J. Neurophysiol. 80, 1–27.

8. Ikemoto, S., and Wise, R.A. (2004). Mapping of chemical trigger zones for reward. Neuropharmacology 47 (Suppl 1), 190–201.

9. Ikemoto, S. (2010). Brain reward circuitry beyond the mesolimbic dopamine system: a neurobiological theory. Neurosci. Biobehav. Rev. 35, 129–150.

10. Olds, J., and Milner, P. (1954). Positive reinforcement produced by electrical stimulation of septal area and other regions of rat brain. J. Comp. Physiol. Psychol. 47, 419–427.

11. Carlezon, W.A., Jr., and Chartoff, E.H. (2007). Intracranial self-stimulation (ICSS) in rodents to study the neurobiology of motivation. Nat. Protoc. 2, 2987–2995.

12. Ikemoto, S. (2007). Dopamine reward circuitry: two projection systems from the ventral midbrain to the nucleus accumbens-olfactory tubercle complex. Brain Res. Brain Res. Rev. 56, 27–78.

13. Wesson, D.W., and Wilson, D.A. (2011). Sniffing out the contributions of the olfactory tubercle to the sense of smell: hedonics, sensory integration, and more? Neurosci. Biobehav. Rev. 35, 655–668.

14. Agustín-Pavón, C., Martínez-García, F., and Lanuza, E. (2014). Focal lesions within the ventral striato-pallidum abolish attraction for male chemosignals in female mice. Behav. Brain Res. 259, 292–296.

15. DiBenedictis, B.T., Olugbemi, A.O., Baum, M.J., and Cherry, J.A. (2015). DREADD-Induced Silencing of the Medial Olfactory Tubercle Disrupts the Preference of Female Mice for Opposite-Sex Chemosignals(1,2,3). eNeuro 2, https://doi.org/10.1523/ENEURO.0078-15.2015.

16. Gadziola, M.A., Tylicki, K.A., Christian, D.L., and Wesson, D.W. (2015). The olfactory tubercle encodes odor valence in behaving mice. J. Neurosci. 35, 4515–4527.

17. Murata, K., Kanno, M., Ieki, N., Mori, K., and Yamaguchi, M. (2015). Mapping of Learned Odor-Induced Motivated Behaviors in the Mouse Olfactory Tubercle. J. Neurosci. 35, 10581–10599.

18. Renier, N., Wu, Z., Simon, D.J., Yang, J., Ariel, P., and Tessier-Lavigne, M. (2014). iDISCO: a simple, rapid method to immunolabel large tissue samples for volume imaging. Cell 159, 896–910.

19. Kobayakawa, K., Kobayakawa, R., Matsumoto, H., Oka, Y., Imai, T., Ikawa, M., Okabe, M., Ikeda, T., Itohara, S., Kikusui, T., et al. (2007). Innate versus learned odour processing in the mouse olfactory bulb. Nature 450, 503–508.

20. Mandairon, N., Poncelet, J., Bensafi, M., and Didier, A. (2009). Humans and mice express similar olfactory preferences. PLoS ONE 4, e4209.

21. Mandairon, N., Sultan, S., Rey, N., Kermen, F., Moreno, M., Busto, G., Farget, V., Messaoudi, B., Thevenet, M., and Didier, A. (2009). A computer-assisted odorized hole-board for testing olfactory perception in mice. J. Neurosci. Methods 180, 296–303.

22. Midroit, M., Thevenet, M., Fournel, A., Sacquet, J., Bensafi, M., Breton, M., Chalençon, L., Cavelius, M., Didier, A., and Mandairon, N. (2018). Non-imaged based method for matching brains in a common anatomical space for cellular imagery. J. Neurosci. Methods 304, 136–145.

23. Tahsili-Fahadan, P., Yahyavi-Firouz-Abadi, N., Khoshnoodi, M.A., Motiei-Langroudi, R., Tahaei, S.A., Ghahremani, M.H., and Dehpour, A.R. (2006). Agmatine potentiates morphine-induced conditioned place preference in mice: modulation by alpha2-adrenoceptors. Neuropsychopharmacology 31, 1722–1732.

24. Huston, J.P., Silva, M.A. de S., Topic, B., and Müller, C.P. (2013). What's conditioned in conditioned place preference? Trends Pharmacol. Sci. 34, 162–166.

25. McReynolds, J.R., Taylor, A., Vranjkovic, O., Ambrosius, T., Derricks, O., Nino, B., Kurtoglu, B., Wheeler, R.A., Baker, D.A., Gasser, P.J., and Mantsch, J.R. (2017). Corticosterone Potentiation of Cocaine-Induced Reinstatement of Conditioned Place Preference in Mice is Mediated by Blockade of the Organic Cation Transporter 3. Neuropsychopharmacology 42, 757–765.

26. Nazarian, A., Russo, S.J., Festa, E.D., Kraish, M., and Quinones-Jenab, V. (2004). The role of D1 and D2 receptors in the cocaine conditioned place preference of male and female rats. Brain Res. Bull. 63, 295–299.

27. Pina, M.M., and Cunningham, C.L. (2014). Effects of dopamine receptor antagonists on the acquisition of ethanol-induced conditioned place preference in mice. Psychopharmacology (Berl.) 231, 459–468.

28. Schindler, C.W., and Carmona, G.N. (2002). Effects of dopamine agonists and antagonists on locomotor activity in male and female rats. Pharmacol. Biochem. Behav. 72, 857–863.

29. Astur, R.S., Carew, A.W., and Deaton, B.E. (2014). Conditioned place preferences in humans using virtual reality. Behav. Brain Res. 267, 173–177.

30. Childs, E., and de Wit, H. (2009). Amphetamine-induced place preference in humans. Biol. Psychiatry 65, 900–904.

31. Licon, C.C., Manesse, C., Dantec, M., Fournel, A., and Bensafi, M. (2018). Pleasantness and trigeminal sensations as salient dimensions in organizing the semantic and physiological spaces of odors. Sci. Rep. 8, 8444.

32. Joussain, P., Thevenet, M., Rouby, C., and Bensafi, M. (2013). Effect of aging on hedonic appreciation of pleasant and unpleasant odors. PLoS ONE 8, e61376.

33. Swanson, L.W. (1982). The projections of the ventral tegmental area and adjacent regions: a combined fluorescent retrograde tracer and immunofluorescence study in the rat. Brain Res. Bull. 9, 321–353.

34. Morales, M., and Margolis, E.B. (2017). Ventral tegmental area: cellular heterogeneity, connectivity and behaviour. Nat. Rev. Neurosci. 18, 73–85.

35. Phillips, A.G., and Mogenson, G.J. (1969). Self-Stimulation of the Olfactory Bulb. Physiol. Behav. 4, 195–197.

36. Imaizumi, M., Takeda, M., and Fushiki, T. (2000). Effects of oil intake in the conditioned place preference test in mice. Brain Res. 870, 150–156.

37. Domínguez-Salazar, E., Naser, H.F., and Velázquez-Moctezuma, J. (2014). D1-like antagonist blocks conditioned place preference induced by ejaculation in male rats. Behav. Brain Res. 269, 15–19.

38. Xiong, A., and Wesson, D.W. (2016). Illustrated Review of the Ventral Striatum's Olfactory Tubercle. Chem. Senses 41, 549–555.

39. Fitzgerald, B.J., Richardson, K., and Wesson, D.W. (2014). Olfactory tubercle stimulation alters odor preference behavior and recruits forebrain reward and motivational centers. Front. Behav. Neurosci. 8, 81.

40. Zhang, Z., Zhang, H., Wen, P., Zhu, X., Wang, L., Liu, Q., Wang, J., He, X., Wang, H., and Xu, F. (2017). Whole-Brain Mapping of the Inputs and Outputs of the Medial Part of the Olfactory Tubercle. Front. Neural Circuits 11, 52.

41. Imamura, F., Ayoub, A.E., Rakic, P., and Greer, C.A. (2011). Timing of neurogenesis is a determinant of olfactory circuitry. Nat. Neurosci. 14, 331–337.

42. Zelano, C., Montag, J., Johnson, B., Khan, R., and Sobel, N. (2007). Dissociated representations of irritation and valence in human primary olfactory cortex. J. Neurophysiol. 97, 1969–1976.

43. de Araujo, I.E., Rolls, E.T., Velazco, M.I., Margot, C., and Cayeux, I. (2005). Cognitive modulation of olfactory processing. Neuron 46, 671–679.

44. Sobel, N., Prabhakaran, V., Zhao, Z., Desmond, J.E., Glover, G.H., Sullivan, E.V., and Gabrieli, J.D. (2000). Time course of odorant-induced activation in the human primary olfactory cortex. J. Neurophysiol. 83, 537–551.

45. Weismann, M., Yousry, I., Heuberger, E., Nolte, A., Ilmberger, J., Kobal, G., Yousry, T.A., Kettenmann, B., and Naidich, T.P. (2001). Functional

Current Biology
Article

CellPress

magnetic resonance imaging of human olfaction. Neuroimaging Clin. N. Am. *11*, 237–250, viii.

46. Zhou, G., Lane, G., Cooper, S.L., Kahnt, T., and Zelano, C. (2019). Characterizing functional pathways of the human olfactory system. eLife *8*, https://doi.org/10.7554/eLife.47177.

47. Hasselmo, M.E., Wilson, M.A., Anderson, B.P., and Bower, J.M. (1990). Associative memory function in piriform (olfactory) cortex: computational modeling and neuropharmacology. Cold Spring Harb. Symp. Quant. Biol. *55*, 599–610.

48. Wilson, D.A. (1998). Habituation of odor responses in the rat anterior piriform cortex. J. Neurophysiol. *79*, 1425–1440.

49. Barkai, E., and Saar, D. (2001). Cellular correlates of olfactory learning in the rat piriform cortex. Rev. Neurosci. *12*, 111–120.

50. Illig, K.R., and Haberly, L.B. (2003). Odor-evoked activity is spatially distributed in piriform cortex. J. Comp. Neurol. *457*, 361–373.

51. Kadohisa, M., and Wilson, D.A. (2006). Separate encoding of identity and similarity of complex familiar odors in piriform cortex. Proc. Natl. Acad. Sci. USA *103*, 15206–15211.

52. Barnes, D.C., Hofacer, R.D., Zaman, A.R., Rennaker, R.L., and Wilson, D.A. (2008). Olfactory perceptual stability and discrimination. Nat. Neurosci. *11*, 1378–1380.

53. Li, W., Howard, J.D., Parrish, T.B., and Gottfried, J.A. (2008). Aversive learning enhances perceptual and cortical discrimination of indiscriminable odor cues. Science *319*, 1842–1845.

54. Howard, J.D., Plailly, J., Grueschow, M., Haynes, J.-D., and Gottfried, J.A. (2009). Odor quality coding and categorization in human posterior piriform cortex. Nat. Neurosci. *12*, 932–938.

55. Gottfried, J.A., Deichmann, R., Winston, J.S., and Dolan, R.J. (2002). Functional heterogeneity in human olfactory cortex: an event-related functional magnetic resonance imaging study. J. Neurosci. *22*, 10819–10828.

56. Sevelinges, Y., Gervais, R., Messaoudi, B., Granjon, L., and Mouly, A.-M. (2004). Olfactory fear conditioning induces field potential potentiation in rat olfactory cortex and amygdala. Learn. Mem. *11*, 761–769.

57. Li, W., Luxenberg, E., Parrish, T., and Gottfried, J.A. (2006). Learning to smell the roses: experience-dependent neural plasticity in human piriform and orbitofrontal cortices. Neuron *52*, 1097–1108.

58. Bensafi, M., Sobel, N., and Khan, R.M. (2007). Hedonic-specific activity in piriform cortex during odor imagery mimics that during odor perception. J. Neurophysiol. *98*, 3254–3262.

59. Sevelinges, Y., Sullivan, R.M., Messaoudi, B., and Mouly, A.-M. (2008). Neonatal odor-shock conditioning alters the neural network involved in odor fear learning at adulthood. Learn. Mem. *15*, 649–656.

60. Barnes, D.C., Chapuis, J., Chaudhury, D., and Wilson, D.A. (2011). Odor fear conditioning modifies piriform cortex local field potentials both during conditioning and during post-conditioning sleep. PLoS ONE *6*, e18130.

61. Pantazopoulos, H., Dolatshad, H., and Davis, F.C. (2011). A fear-inducing odor alters PER2 and c-Fos expression in brain regions involved in fear memory. PLoS ONE *6*, e20658.

62. Schoenbaum, G., and Eichenbaum, H. (1995). Information coding in the rodent prefrontal cortex. I. Single-neuron activity in orbitofrontal cortex compared with that in pyriform cortex. J. Neurophysiol. *74*, 733–750.

63. Litaudon, P., Mouly, A.M., Sullivan, R., Gervais, R., and Cattarelli, M. (1997). Learning-induced changes in rat piriform cortex activity mapped using multisite recording with voltage sensitive dye. Eur. J. Neurosci. *9*, 1593–1602.

64. Cohen, Y., Reuveni, I., Barkai, E., and Maroun, M. (2008). Olfactory learning-induced long-lasting enhancement of descending and ascending synaptic transmission to the piriform cortex. J. Neurosci. *28*, 6664–6669.

65. Gottfried, J.A. (2010). Central mechanisms of odour object perception. Nat. Rev. Neurosci. *11*, 628–641.

66. Wilson, D.A., and Sullivan, R.M. (2011). Cortical processing of odor objects. Neuron *72*, 506–519.

67. Berridge, K.C., Robinson, T.E., and Aldridge, J.W. (2009). Dissecting components of reward: 'liking', 'wanting', and learning. Curr. Opin. Pharmacol. *9*, 65–73.

68. Salimpoor, V.N., Benovoy, M., Larcher, K., Dagher, A., and Zatorre, R.J. (2011). Anatomically distinct dopamine release during anticipation and experience of peak emotion to music. Nat. Neurosci. *14*, 257–262.

69. Ferreri, L., Mas-Herrero, E., Zatorre, R.J., Ripollés, P., Gomez-Andres, A., Alicart, H., Olivé, G., Marco-Pallarés, J., Antonijoan, R.M., Valle, M., et al. (2019). Dopamine modulates the reward experiences elicited by music. Proc. Natl. Acad. Sci. USA *116*, 3793–3798.

70. Lacey, S., Hagtvedt, H., Patrick, V.M., Anderson, A., Stilla, R., Deshpande, G., Hu, X., Sato, J.R., Reddy, S., and Sathian, K. (2011). Art for reward's sake: visual art recruits the ventral striatum. Neuroimage *55*, 420–433.

71. Yu, X., Li, W., Ma, Y., Tossell, K., Harris, J.J., Harding, E.C., Ba, W., Miracca, G., Wang, D., Li, L., et al. (2019). GABA and glutamate neurons in the VTA regulate sleep and wakefulness. Nat. Neurosci. *22*, 106–119.

72. Yoshihara, S., Omichi, K., Yanazawa, M., Kitamura, K., and Yoshihara, Y. (2005). Arx homeobox gene is essential for development of mouse olfactory system. Development *132*, 751–762.

73. Abraham, A., Pedregosa, F., Eickenberg, M., Gervais, P., Mueller, A., Kossaifi, J., Gramfort, A., Thirion, B., and Varoquaux, G. (2014). Machine learning for neuroimaging with scikit-learn. Front. Neuroinformatics *8*, https://doi.org/10.3389/fninf.2014.00014.

74. Esteban, O., Markiewicz, C.J., Blair, R.W., Moodie, C.A., Isik, A.I., Erramuzpe, A., Kent, J.D., Goncalves, M., DuPre, E., Snyder, M., et al. (2019). fMRIPrep: a robust preprocessing pipeline for functional MRI. Nat. Methods *16*, 111–116.

75. Gorgolewski, K., Burns, C.D., Madison, C., Clark, D., Halchenko, Y.O., Waskom, M.L., and Ghosh, S.S. (2011). Nipype: a flexible, lightweight and extensible neuroimaging data processing framework in python. Front. Neuroinform. *5*, 13.

76. Avants, B.B., Epstein, C.L., Grossman, M., and Gee, J.C. (2008). Symmetric diffeomorphic image registration with cross-correlation: evaluating automated labeling of elderly and neurodegenerative brain. Med. Image Anal. *12*, 26–41.

77. Tustison, N.J., Avants, B.B., Cook, P.A., Zheng, Y., Egan, A., Yushkevich, P.A., and Gee, J.C. (2010). N4ITK: improved N3 bias correction. IEEE Trans. Med. Imaging *29*, 1310–1320.

78. Dielenberg, R.A., Hunt, G.E., and McGregor, I.S. (2001). "When a rat smells a cat": the distribution of Fos immunoreactivity in rat brain following exposure to a predatory odor. Neuroscience *104*, 1085–1097.

79. Kovács, K.J. (2008). Measurement of immediate-early gene activation- c-fos and beyond. J. Neuroendocrinol. *20*, 665–672.

80. Cruz, F.C., Koya, E., Guez-Barber, D.H., Bossert, J.M., Lupica, C.R., Shaham, Y., and Hope, B.T. (2013). New technologies for examining the role of neuronal ensembles in drug addiction and fear. Nat. Rev. Neurosci. *14*, 743–754.

81. Maviel, T., Durkin, T.P., Menzaghi, F., and Bontempi, B. (2004). Sites of neocortical reorganization critical for remote spatial memory. Science *305*, 96–99.

82. Frankland, P.W., Bontempi, B., Talton, L.E., Kaczmarek, L., and Silva, A.J. (2004). The involvement of the anterior cingulate cortex in remote contextual fear memory. Science *304*, 881–883.

83. Okuyama, T., Kitamura, T., Roy, D.S., Itohara, S., and Tonegawa, S. (2016). Ventral CA1 neurons store social memory. Science *353*, 1536–1541.

84. Gradinaru, V., Zhang, F., Ramakrishnan, C., Mattis, J., Prakash, R., Diester, I., Goshen, I., Thompson, K.R., and Deisseroth, K. (2010). Molecular and cellular approaches for diversifying and extending optogenetics. Cell *141*, 154–165.

85. Johnson, K.A., Voyvodic, L., Loewinger, G.C., Mateo, Y., and Lovinger, D.M. (2020). Operant self-stimulation of thalamic terminals in the dorsomedial striatum is constrained by metabotropic glutamate receptor 2. Neuropsychopharmacology *45*, 1454–1462.

86. Cleland, T.A., Morse, A., Yue, E.L., and Linster, C. (2002). Behavioral models of odor similarity. Behav. Neurosci. *116*, 222–231.

87. Kermen, F., Chakirian, A., Sezille, C., Joussain, P., Le Goff, G., Ziessel, A., Chastrette, M., Mandairon, N., Didier, A., Rouby, C., and Bensafi, M. (2011). Molecular complexity determines the number of olfactory notes and the pleasantness of smells. Sci. Rep. *1*, https://doi.org/10.1038/srep00206.

88. Gadziola, M.A., and Wesson, D.W. (2016). The Neural Representation of Goal-Directed Actions and Outcomes in the Ventral Striatum's Olfactory Tubercle. J. Neurosci. *36*, 548–560.

89. Mandairon, N., Kuczewski, N., Kermen, F., Forest, J., Midroit, M., Richard, M., Thevenet, M., Sacquet, J., Linster, C., and Didier, A. (2018). Opposite regulation of inhibition by adult-born granule cells during implicit versus explicit olfactory learning. eLife *7*, https://doi.org/10.7554/eLife.34976.

90. Hietala, J., Seppälä, T., Lappalainen, J., and Syvälahti, E. (1992). Quantification of SCH 39166, a novel selective D1 dopamine receptor antagonist, in rat brain and blood. Psychopharmacology (Berl.) *106*, 455–458.

91. Hegoburu, C., Sevelinges, Y., Thévenet, M., Gervais, R., Parrot, S., and Mouly, A.-M. (2009). Differential dynamics of amino acid release in the amygdala and olfactory cortex during odor fear acquisition as revealed with simultaneous high temporal resolution microdialysis. Learn. Mem. *16*, 687–697.

92. Richard, S., Aguilera, N., Thévenet, M., Dkhissi-Benyahya, O., and Flamant, F. (2017). Neuronal expression of a thyroid hormone receptor α mutation alters mouse behaviour. Behav. Brain Res. *321*, 18–27.

93. Sezille, C., Messaoudi, B., Bertrand, A., Joussain, P., Thévenet, M., and Bensafi, M. (2013). A portable experimental apparatus for human olfactory fMRI experiments. J. Neurosci. Methods *218*, 29–38.

94. Fonov, V., Evans, A., McKinstry, R., Almli, C., and Collins, D. (2009). Unbiased nonlinear average age-appropriate brain templates from birth to adulthood. Neuroimage *47*, S102.

95. Zhang, Y., Brady, M., and Smith, S. (2001). Segmentation of brain MR images through a hidden Markov random field model and the expectation-maximization algorithm. IEEE Trans. Med. Imaging *20*, 45–57.

96. Cox, R.W. (1996). AFNI: software for analysis and visualization of functional magnetic resonance neuroimages. Comput. Biomed. Res. *29*, 162–173.

97. Jenkinson, M. (2003). Fast, automated, N-dimensional phase-unwrapping algorithm. Magn. Reson. Med. *49*, 193–197.

98. Greve, D.N., and Fischl, B. (2009). Accurate and robust brain image alignment using boundary-based registration. Neuroimage *48*, 63–72.

99. Behzadi, Y., Restom, K., Liau, J., and Liu, T.T. (2007). A component based noise correction method (CompCor) for BOLD and perfusion based fMRI. Neuroimage *37*, 90–101.

100. Power, J.D., Mitra, A., Laumann, T.O., Snyder, A.Z., Schlaggar, B.L., and Petersen, S.E. (2014). Methods to detect, characterize, and remove motion artifact in resting state fMRI. Neuroimage *84*, 320–341.

101. Zelano, C., Bensafi, M., Porter, J., Mainland, J., Johnson, B., Bremner, E., Telles, C., Khan, R., and Sobel, N. (2005). Attentional modulation in human primary olfactory cortex. Nat. Neurosci. *8*, 114–120.

102. Moreno, M.M., Linster, C., Escanilla, O., Sacquet, J., Didier, A., and Mandairon, N. (2009). Olfactory perceptual learning requires adult neurogenesis. Proc. Natl. Acad. Sci. USA *106*, 17980–17985.

103. Mandairon, N., Sultan, S., Nouvian, M., Sacquet, J., and Didier, A. (2011). Involvement of newborn neurons in olfactory associative learning? The operant or non-operant component of the task makes all the difference. J. Neurosci. *31*, 12455–12460.

104. Sultan, S., Rey, N., Sacquet, J., Mandairon, N., and Didier, A. (2011). Newborn neurons in the olfactory bulb selected for long-term survival through olfactory learning are prematurely suppressed when the olfactory memory is erased. J. Neurosci. *31*, 14893–14898.

105. Moreno, M.M., Bath, K., Kuczewski, N., Sacquet, J., Didier, A., and Mandairon, N. (2012). Action of the noradrenergic system on adult-born cells is required for olfactory learning in mice. J. Neurosci. *32*, 3748–3758.

Current Biology
Article

 CellPress

STAR★METHODS

KEY RESOURCES TABLE

REAGENT or RESOURCE	SOURCE	IDENTIFIER
Antibodies		
anti-c-Fos	Santa Cruz Biotechnology	Cat# sc-189; RRID:AB_2231020
chicken anti-EYFP	Anaspec TEBU	Cat# 55423; RRID:AB_1657428
chicken anti-TH	Abcam	Cat# ab76442; RRID:AB_1524535
rabbit anti-c-Fos	Proteintech	Cat# 26192; N/A
anti-DARPP-32	Abcam	Cat# ab40801; RRID:AB_731843
mouse anti-c-Fos	Proteintech	Cat# 66590-1-Ig; RRID:AB_2881950
guinea pig anti-Tbx21	[72]	N/A
rabbit anti-EYFP	Millipore	Cat# AB3080P; RRID:AB_2630379
Bacterial and Virus Strains		
Lenti-hSyn-eNpHR3.0-EYFP lentivirus	Addgene	RRID:Addgene_26775
Control Lenti-hSyn-EYFP lentivirus	[6]	N/A
Chemicals, Peptides, and Recombinant Proteins		
R(+)-SCH-23390 hydrochloride	Addgene	RRID:AB_11159773
Deposited Data		
Analyzed data	This paper	https://github.com/Neuropop/Reward2021
Experimental Models: Organisms/Strains		
C57Bl6J	Charles River Laboratories	Cat# JAX:000664, RRID:IMSR_JAX:000664
Software and Algorithms		
Statistica	Statistica	https://www.statistica.com
Volcan	[22]	N/A
NiLearn	NiLearn [73]	http://nilearn.github.io
SciPy	Python Library	http://www.scipy.org/; RRID:SCR_008058
MRIcron	MRIcron	http://www.mricro.com
fMRIPrep	[74]	https://fmriprep.org
Nipype	[75]	https://nipype.readthedocs.io
SPM	MATLAB Toolbox	https://www.fil.ion.ucl.ac.uk/spm/
FSL	FMRIB Software Library	https://fsl.fmrib.ox.ac.uk
ANTS	[76]	http://stnava.github.io/ANTs/; RRID:SCR_004757
MATLAB	Mathworks	https://www.mathworks.com/products/matlab.html RRID:SCR_001622

RESOURCES AVAILABILITY

Lead contact
Further information and requests for resources and reagents should be directed to and will be fulfilled by the Lead Contact, Nathalie Mandairon (nathalie.mandaiorn@cnrs.fr).

Materials availability
This study did not generate new unique reagents.

Data and code availability
The datasets and codes generated during this study have been deposited: https://github.com/Neuropop/Reward2021.

EXPERIMENTAL MODEL AND SUBJECT DETAILS

For all *in vivo* animal studies, we used 145 adult male C57Bl6/J mice (Charles River Laboratories, L'Arbresle, France) aged of 2 months at the beginning of the experiments. Experiments were done following procedures in accordance with the European Community Council Directive of 22nd September 2010 (2010/63/UE) and the National Ethics Committee (Agreement DR2013-48 (vM)). Mice were kept on a 12 h light/dark cycle (22°C) with food and water *ad libitum*. Mouse assignation to the various experimental groups was randomized. Mice were housed by group of 5, then individually after surgery. All experiments were conducted after at least 1 week of habituation and handling.

For human studies, the data were collected and treated according to the ethical guidelines of the Declaration of Helsinki and approved by French IdF-IV ethics committee (CPP study) and by the Lyon Sud-Est ethics committee (fRMI study). All participants were recruited from the Lyon area in France. Their olfactory performances were verified using the European Test of Olfactory Capabilities.[77] All participants received financial compensation for the experiment and provided written informed consent prior to participation. Participant assignation to the various experimental groups was randomized. For CPP study, 72 participants were tested in total but 2 were excluded due to olfactory pollution and 1 left the living lab during the experiment. Thus, only 69 participants (34 women, 35 men) between the ages of 18 and 30 years (mean ± SD, 21.5 ± 2.6 years) provided data from April to May 2018. For fRMI study, 30 participants were tested (15 women, 15 men) between the ages of 19 and 34 years (means ± SD, 22.4 ± 3.5 years).

METHOD DETAILS

Cell analysis

Mice were sacrificed 1 h after odor stimulation or behavioral test using pentobarbital (0.2 mL/30 g) or dolethal (0.1 mL/30 g) and intracardiac perfusion of 50 mL of fixative (PFA 4%, pH = 7.4). This 1 h delay has previously been shown to enable the expression of the immediate early gene c-Fos in response to odorant stimulation,[78,79] allowing the mapping of neuronal activation.[6,78–83] The brains were removed, post-fixed overnight, cryoprotected in sucrose (20%), frozen rapidly, and then stored at −20°C before sectioning with a cryostat (14 μm thick; 210 μm intervals). After immunohistochemistries using fluorescent secondary antibodies, sections were then coverslipped in Vectashield combined with DAPI (Vector laboratories). All fluorescent counting was done blind with regards to the identity of the animal and using AxioVision (Zeiss) software coupled to a fluorescent pseudo-confocal Zeiss microscope.

Optogenetic intracranial self-stimulation

Electric intracranial self-stimulation has been extensively used to determine brain areas belonging to the reward system and unravel the neural bases of motivation.[10,11] This technic consists in an operant conditioning in which the stimulation of a specific brain area serves as reinforcer.

Lentivirus injection and optical fiber implantation in the olfactory bulb

Prior to surgery, 24 mice were anaesthetized with an intraperitoneal cocktail injection of 50 mg/kg ketamine and 7.5 mg/kg xylazine and secured in a stereotaxic instrument (Narishige Scientific Instruments, Tokyo, Japan). 150 nL of Lenti-hSyn-eNpHR3.0-EYFP lentivirus (9.22 × 10⁶ IU/mL, expressing halorhodopsin and the yellow fluorescent protein) were injected bilaterally in pOB (with respect to the bregma: AP, +4.3 mm; ML, ± 0.75; DV, −2 mm; n = 7), and in the aOB (with respect to the bregma: AP, +5 mm; ML, ± 0.75; DV, −2 mm; n = 9). 300 nL of control Lenti-hSyn-EYFP lentivirus (1.1 × 10⁶ IU/mL, expressing only EYFP; n = 9) were injected bilaterally in pOB at the rate of 150 nL/min. Following virus infusions, a dual optical fiber (200-nm core diameter, 0.22 N.A.; Doric Lenses) was implanted into the OB at the same coordinates as the virus infusion. The pLenti-hSyn-eNpHR 3.0-EYFP was a gift from Karl Deisseroth[84] and obtained through Addgene (plasmid #26775). Generation of the control Lenti-hSyn-EYFP lentivirus (empty virus containing only the EYFP insert) has been described previously.[6]

Optical self-stimulation in freely moving animals

8 weeks after surgery, mice underwent the conditioning phases in which they were allowed to move freely on the one-hole-board apparatus for 2-min trial during 5 days. The bilateral continuous light stimulation (crystal laser, 561 nm, 10–15 mW) was automatically triggered by the entry of the mouse's nose within 1 cm (light-triggering zone) of the hole (VideoTrack, Viewpoint) and lasted as long as the nose poke, mimicking odor investigation. This phase was followed by an extinction phase in which the nose presence in the zone did not trigger light stimulation anymore (5 trials on 3 days) and one last session in which light stimulation was available again similarly as in the previous conditioning phase.[85] Total duration of time spent by the nose in the zone was recorded.

Cellular analysis

Mice were sacrificed one h after a behavioral session in which light stimulation was available. Behavioral performances of this session were not different from those of the last behavioral session (Light1') (Bonferroni corrected Two-Tailed Wilcoxon for difference between session of the day of sacrifice and Light1', NpHR post group: p = 0.094; EYFP post group: p = 1; NpHR ant group p = 1).

OB sections were double labeled after immunohistochemistries against EYFP and c-Fos proteins to control the effect of light stimulation on transfected granule cells. Briefly, rabbit anti-c-Fos (1:5000; Santa Cruz Biotechnology, Santa Cruz, CA, USA, ref: Sc-189) and chicken anti-EYFP (1:1000; Anaspec TEBU, ref: 55423) primary antibodies were combined respectively with Alexa 546 goat anti-rabbit (1:250; Vector Laboratories, Burlingame, CA, USA) and Alexa 488 goat anti-chicken (1:250; Molecular Probes) antibodies. The total density of EYFP⁺ and the percentage of double-labeled cells (EYFP⁺/c-Fos⁺) were assessed in the ventral OB at the level of the

Current Biology
Article

injection site (2 sections/animal) and at 0.96 mm from the injection site along the antero-posterior axis (2 sections/animal) (aBO; coordinates from the bregma [+5.33 to +4.73]; pOB: coordinates from the bregma [+4.61 to +3.89]).

To investigate the activity of the VTA (coordinate from the bregma [-3.3]) after self-stimulation, immunohistochemistries against TH and c-Fos were performed. Briefly, chicken anti-TH (1:2000; AbCam, ref: 76442) and rabbit anti-c-Fos (1:2000; ProteinTech, ref: 26192) primary antibodies were combined respectively with Alexa 546 goat anti-chicken (1:250; Molecular Probes) and Alexa 488 goat anti-rabbit (1:250; Vector Laboratories, Burlingame, CA, USA) antibodies and the percentage of double-labeled cells (TH+/c-Fos+) was counted (one section/animal; 10-32 cells/animal).

To investigate the activity of medium spiny neurons of the OT (coordinates from the bregma [+2.09 to −0.11]) after self-stimulation behavior, immunohistochemistries against DARPP-32 and c-Fos were performed. DARPP-32 has been used as a marker of medium spiny neurons of the striatum and the OT.[17] Briefly, rabbit anti-DARPP-32 (1:500; AbCam, ref: 40801) and mouse anti-c-Fos (1:500; ProteinTech, ref: 66590) primary antibodies were combined respectively with Alexa 488 goat anti-rabbit (1:250; Molecular Probes) and Alexa 546 goat anti-mouse (1:250; Molecular Probes) antibodies. The percentage of double-labeled cells (DARPP-32+/c-Fos+) was counted on five OT sections per animal (200-285 cells/animal).

Statistics

Because of the lack of sphericity on behavioral data, we used Friedman test, non-parametric alternative to the repeated-measures ANOVA, for trial effect, and Wilcoxon, non-parametric test equivalent to the t-test, for specific trial comparisons. The location and the efficiency of viral infection were controlled using Bonferroni corrected One-Tailed Paired t-tests. Mann-Whitney tests were used for VTA and OT activities between group comparisons.

iDISCO
Viral injection

Prior to surgery, 16 mice were anaesthetized and secured in a stereotaxic instrument as described previously. 150 nL of Lenti-hSyn-eNpHR3.0-EYFP lentivirus ($9,22 \times 10^6$ IU/mL, expressing halorhodopsin and the yellow fluorescent protein) was injected bilaterally in pOB (with respect to the bregma: AP, +4.3 mm; ML, ± 0.75; DV, −2,8 mm; n = 8) or in aOB (with respect to the bregma: AP, +5 mm; ML, ± 0.75; DV, −2 mm; n = 8) at the rate of 150 nL/min.

iDISCO+ processing and light-sheet microscopy

Six brains were dehydrated in baths of methanol in ddH2O in a concentration gradient (20%, 40% 60%, 80% and 100% twice), and then put in methanol / DiChloroMethane (DCM) 1:2 overnight. Samples were then washed all day in methanol, and then bleached with 5% H_2O_2 (1 volume of 30% H_2O_2 for 5 volumes of methanol, ice cold) at 4°C overnight. Then samples were re-equilibrated at room temperature slowly and re-hydrated in baths of methanol in H_2O at different concentration during one h each (80%, 60%, 40% and 20%) and finally in PBS/0.2% Triton X-100 for 1 h twice.

Pre-treated samples were then incubated in PBS/0.2% Triton X-100/20% DMSO/0.3M glycine at 37°C for 36 h, then blocked in PBS/0.2% Triton X-100/10% DMSO/2% Porc Skin Gelatin at 37°C for 2 days. Samples were then incubated in primary antibodies: chicken anti-GFP (1:2000, Aves GFP-1020) in PBS-Tween 0.2% with heparin 10 mg/mL (PTwH)/5% DMSO/3% donkey serum at 37°C for 4 to 7 days. Samples were then washed in PTwH for 24 h (five changes of the PTwH solution over that time), then incubated in secondary antibody donkey anti-chicken (Jackson Immunoresearch at 1:500 in PTwH/3% donkey serum) at 37°C for 4 to 7 days. Samples were finally washed in PTwH for 1 day before clearing and imaging. Immunolabelled brains were dehydrated in baths of methanol in ddH2O at different concentrations (20%, 40% 60%, 80% and 100% twice). Samples were incubated overnight in 1 vol of methanol/2 vol of dichloromethane (DCM, Sigma-Aldrich 270997-12 × 100 ML) (Eppendorf tubes were used throughout the process).

The methanol was then washed for 20 min twice in 100% DCM. Finally, samples were incubated (without shaking) in dibenzyl ether (DBE, Sigma-Aldrich 108014–1 KG) until clear and then stored in DBE at room temperature.

Cleared samples were imaged in sagittal orientation (right lateral side up) on a light-sheet microscope (Ultramicroscope II, LaVision Biotec, Germany) equipped with a sCMOS camera (Andor Neo, UK) and 4X/0.3 objective. A numerical aperture of 0.6 was used for the light sheet, with a fixed 3-sources illumination. The microscope is equipped with LED lasers (488 nm and 640 nm).

Emission filters used are 525/50 and 680/30. The samples were scanned with a step-size of 3 μm.

3D projections were performed using Imaris (Bitplane, http://www.bitplane.com/imaris/imaris). Images in Figures 2A and 2B were obtained from two brains.

Quantification of OB-OT neural projections

On the 10 remaining brains, coronal sections were performed. OB sections were double labeled by immunohistochemistries against Tbx21 (marker of mitral cells) and EYFP. Briefly, guinea pig anti-Tbx21 (1:5000, gift from Y. Yoshihara[72]) and rabbit anti-EYFP (1:1000; Merk, ref: AB3080) primary antibodies were combined respectively with Alexa 546 goat anti-guinea pig (1:250; Molecular Probes) and Alexa 488 goat anti-rabbit (1:250; Vector Laboratories, Burlingame, CA, USA) antibodies. The percentage of double-labeled cells (Tbx21+/EYFP+) was assessed in the ventral OB over 3 sections at the injection site and at 0.96 mm from the injection site along the antero-posterior axis.

OT and PirCX sections (aPirCX: coordinates from the bregma [+2.33 to +1.09]; pPirCX: coordinates from the bregma [-0.23 to −2.79]) were labeled by immunohistochemistry of EYFP proteins as described previously. ImageJ was used to define a threshold for each image acquired by AxioVision and we calculated the percentage of labeled area (% labeled area = labeled area/total area*100).

Statistics

Bonferroni corrected Mann-Whitney tests were performed for pOB versus aOB labeled area comparisons. The percentage of $Tbx21^+$/c-Fos^+ cells was compared between the injection site in the OB and the antero-posterior opposite side using Bonferroni corrected Wilcoxon tests and between groups comparison was done using Mann-Whitney. One-Tailed Unpaired t-test was performed for parametric data.

c-Fos mapping of the olfactory secondary areas

Odorants

Six monomolecular odorants were used: three highly attractive (LIM, CAM and CITRO) versus three poorly attractive (PYR, GUA and CRE) diluted at 1Pa in mineral oil. Mineral oil was used as control[6,86,87] (Table S1).

Behavioral assessment of odor attraction

Odor attraction was measured in 30 mice using odor investigation time.[6,19,20] As previously described,[6] we used a computer-assisted one-hole-board apparatus fitted with sensors to automatically monitor the duration of nose poking into the central hole.[20,21] Total duration of nose poking into the hole was used as a measure of odor attraction. A polypropylene swab impregnated with 60 µL of odorant was placed at the bottom of the hole, under a grid covered with clean bedding. The bedding was replaced after each trial. Every animal was allowed to explore each of the 6 odorants and a no odor condition (60 µL of mineral oil) for 2 min. Each animal tested one odorant per day. Odorants were randomly presented and animals performed no more than 2 consecutive days of testing.

Odor stimulation and sacrifice

Mice were submitted to odor stimulation one h before sacrifice. Briefly, mice were first placed in individual clean cages for 1 h, with an empty tea ball hanging from the top of the cage. A polypropylene swab impregnated with one odorant (60µL, 1Pa) was then placed in the tea ball for a further h.

c-Fos immunohistochemistry

A rabbit anti-c-Fos primary antibody was used (1:5000; Santa Cruz Biotechnology, Santa Cruz, CA, USA) and combined to bio-tinylated goat anti-rabbit (1:200; Vector Laboratories, Burlingame, CA, USA). Brain sections were then processed through an avidin–biotin–peroxidase complex (ABC Elite Kit, Vector Laboratories). Following dehydratation in graded ethanols, sections were defatted in xylene and coverslipped in DPX (Fluka, Sigma).

c-Fos-positive cell mapping

We used a method consisting in a high-accuracy matching of experimental brain sections with a reference brain atlas.[22] It allows precise, automatic assignment of the labeled cells to a brain structure and permits between-group comparisons. Briefly, for each animal, c-Fos immunohistochemistry was performed on brain adjacent sections (n = 6-7 mice for each hedonic condition; 210 µm interval inter sections). For each section analyzed, the external contour of the right hemisphere was outlined and c-Fos^+ cells were automatically counted using mapping software (Mercator, Explora Nova, La Rochelle, France) coupled to a Zeiss microscope. Then, the coordinates of each labeled cell (c-Fos^+) and the contour point were exported. All cell counts were conducted blind with regard to the experimental group.

A digitized Paxinos atlas was used as a common anatomical space (« The mouse brain », Paxinos and Franklin's, 4th edition). The extracted contour and labeling of experimental sections were precisely matched to the corresponding atlas sections. More precisely, the extracted sections were automatically stacked, realigned, and reoriented between them and along the antero-posterior axis. Then, a nonlinear elastic registration based on a computed vector field is applied to the labeling and contour allowing a readjustment of the section size and a precise matching in the atlas. At the end of this computation, each labeled c-Fos^+ cell is correctly located in the common Paxinos Atlas and is thus spatially assigned to one region or sub-region. Since the experimental sections have been matched to the atlas, we selected regions of interest and extracted the density of labeled c-Fos^+ cells in this particular region.

Analyses

We analyzed the neural representation of attractive and unattractive odorants in olfactory brain structures directly targeted by the OB: the Accessory Olfactory Nucleus (AON; coordinates from the bregma [+3.53 to +1.97]), the anterior Piriform Cortex (aPirCX; coordinates from the bregma [+2.33 to +1.09]), the posterior Piriform Cortex (pPirCX; coordinates from the bregma [-0.23 to −2.79]), the Olfactory Tubercle (OT; coordinates from the bregma [+2.09 to −0.11]), the postero-lateral Cortical Amygdala (plCoA; coordinates from the bregma [-1.23 to −3.15]) and the Entorhinal Cortex (EntCX; coordinates from the bregma [-1.91 to −3.87]). The OT was divided in medial (mOT) and lateral (lOT) domains. Then, c-Fos^+ cells were automatically counted using mapping software (Mercator, Explora Nova, La Rochelle, France) as previously described.

By considering the odorant treatment given before the sacrifice, 2 groups of mice were formed and compared: attractive group (n = 6) and unattractive group (n = 7). We extracted the density of labeled c-Fos^+ cells for each brain structure and compared it between groups.

Double labeling analysis

To investigate the activity of VTA and OT after free exploration of the odorants, we performed and analyzed immunohistochemistries against TH/c-Fos and DARPP-32/c-Fos as previously described.

Statistics

For behavioral analyses, Friedman test, a non-parametric alternative to the repeated-measures ANOVA, was used to assess odorant attraction effect. The effect was confirming by permutation test (10x100 000 permutations). For c-Fos mapping between group comparisons, Bonferroni corrected One-Tailed Unpaired t-tests were performed. One-Tailed Unpaired t-tests were used for VTA and OT activities between group comparisons.

Current Biology
Article

CellPress

Olfactory tubercle in vivo electrophysiology
Animals
C57BL/6 male mice (n = 15, 2–4 months of age) originating from Envigo were bred and maintained within the Case Western Reserve University School of Medicine animal facility. Mice were housed on a 12 h light/dark cycle with food and water available *ad libitum*. Up to five mice were cohoused in a cage before experimentation, but all postsurgical animals were housed individually. All experimental procedures were conducted in accordance with the guidelines of the National Institutes of Health and were approved by the Case Western Reserve University Institutional Animal Care and Use Committee.

Surgical procedures
Mice were anesthetized with isoflurane (2–4% in oxygen; Abbott Laboratories) and mounted in a Kopf stereotaxic frame with a water-filled heating pad (38°C) beneath to maintain body temperature. Anesthesia depth was verified by the absence of the toe-pinch reflex. An injection of a local anesthetic (10% marcaine, 0.05 ml, s.c.) was administered into the wound margin site before exposing the dorsal skull. A craniotomy was made to access the right medial OT (+1.7 mm from bregma, +0.5 mm lateral). An eight-channel tungsten electrode array, as previously described[16] was implanted within the right medial OT (4.7 mm ventral) and cemented in place. A second craniotomy was made over the contralateral cortex for placement of a stainless steel ground wire. Animals were allowed to recover for 5 days with food and water *ad libitum*. During the first 3 post-operative days, animals received a daily injection of carprofen (5 mg/kg, s.c.; Pfizer Animal Health).

In vivo *electrophysiology*
The output of the electrode array was amplified, digitized at 24.4 kHz and filtered (bandpass filter, 300–3000 Hz) using an Intan 16 channel headstage and an RHD2000 interface board. One electrode wire was selected to serve as a local reference. Given the small dorsal–ventral extent of the OT ($\sim$300 μm), the electrode arrays were fixed in place, and no attempt was made to record from unique populations of neurons on different sessions. Indeed, it is possible that the same neuron was recorded across multiple days. On average, 5.56 ± 0.61 single neurons were recorded per mouse per session, with an average of 1.96 ± 0.08 neurons recorded per viable electrode wire per mouse per session. After all recording sessions were completed, mice were given (intraperitoneally) an overdose of Fatal-plus and were transcardially perfused with 0.9% saline and 10% formalin, and brains stored in 30% sucrose formalin at 4°C. OT recording sites (targeting the medial portion of the OT) were verified by histological examinations of slide-mounted, 40 μm coronal sections stained with a 1% cresyl violet solution. 5 animals did not contribute data since the recording sites were not located in the mOT.

Analysis of odor-evoked activity
Single units were identified offline in Spike2 (Cambridge Electronic Design), using a combination of template matching and cluster cutting based on principal component analysis.[16] Single units were further defined as those having < 2% of the spikes occurring within a refractory period of 2 ms. Among these identified single units, spike times associated with each odor condition were subsequently extracted for analysis.

For each neuron, we quantified the number of spikes during the 120 s of the trial. The numbers of spikes obtained for the three attractive and for the three unattractive odorants were averaged across neurons to reveal the activity reflecting attraction to odorants independently of their identity, as we did for the c-Fos data. To assess modulations in firing rate according to the attraction condition, spiking was aligned to the first odor investigation (t_0, when the mouse's nose enters the odorized zone). Mean firing rates across trials were measured in 100 ms bins. The mOT neurons fired at a low rate of 3.35 spikes/s (range, 0.05–33 spikes/s across the sampled population), in line with previous studies.[16,88] This firing rate was used as a reference background activity whereas mean odor firing rate for each neuron was calculated over the 3 s time-interval preceding the first investigation, referring to the first approaching phase (-3 to 0 s relative to the onset (t_0) of odor investigation), of attractive and unattractive odorants. Trials in which the animal was already approaching the odorant source at the start of the trial (incomplete -3 s to 0 s period) were removed from the analysis.

Statistics
Between group comparison was performed using Mann-Whitney and difference between Odorized Hole and background was compared using Bonferroni corrected Wilcoxon.

pOB-mOT optogenetic inhibition
Lentivirus injection and optical fiber implantation
Prior to surgery, 17 mice were anesthetized with an intraperitoneal cocktail injection of 50 mg/kg ketamine and 7.5 mg/kg xylazine and secured in a stereotaxic instrument (Narishige Scientific Instruments, Tokyo, Japan). 150 nL of pLenti-hSyn-eNpHR3.0-EYFP lentivirus (9,22 × 106 IU/mL, expressing halorhodopsin and the yellow fluorescent protein; n = 9) or 300nl of control pLenti-hSyn-EYFP lentivirus (1,1 × 106 IU/mL, expressing only EYFP; n = 8) were injected bilaterally in mitral cells layer of the posterior olfactory bulb (with respect to the bregma: AP, +4.3 mm; ML, ± 0.75; DV, −3 mm) at the rate of 150 nL/min. Following virus infusions, a dual optical fiber (200-nm core diameter, 0.22 N.A.; Doric Lenses) was implanted into the mOT with respect to the bregma: AP, +1.7 mm; ML, ± 0.5; DV, −4.7 mm).

Optical inhibition of pOB-mOT pathway
4 weeks after surgery, odorant attraction (LIM, CAM, CITRO, CRE, GUA and PYR) was measured as previously described. The bilateral continuous light stimulation (crystal laser, 561 nm, 10–15 mW) was automatically triggered by mice nose poking within 1 cm (light-triggering zone) of the odorized hole (VideoTrack, Viewpoint) and stopped automatically when the mouse's nose exited the zone.

Control of virus injection location

A few days after optogenetic experiment, mice were sacrificed one h after a 15 min stimulation session (5 s of light stimulation every 15 s for 2 min at 10–15 mW, mimicking the light stimulation received during the olfactory test) as previously described. Double labeling for transfected mitral cells was performed using Tbx21[6,89] and EYFP immunohistochemistry. Briefly, guinea-pig anti-Tbx21 (1:15, 000; gift from Y. Yoshihara[90]) and rabbit anti-EYFP (1:1, 000; Merk, ref: AB3080) primary antibodies were combined respectively with Alexa 546 goat anti-guinea-pig (1:250; Molecular probes) and Alexa 488 goat anti-rabbit (1:250 ; Vector Laboratories, Burlingame, CA, USA) antibodies.

The percentage of double-labeled cells (Tbx21$^+$/EYFP$^+$) was assessed in the ventral OB over 3 sections at the injection site using AxioVision (Zeiss) software coupled to a fluorescent pseudo-confocal Zeiss microscope. Counting was performed blind with regards to the identity of the animal.

Control of pOB-mOT light-inhibition on the OT

To investigate the activity of the OT after optogenetic inhibition of pOB-mOT pathway, we performed and analyzed immunohisto-chemistry against DARPP-32/c-Fos in mOT and lOT as previously described.

Statistics

Between groups comparisons were performed using Mann-Whitney and Spearman test was used for correlation between OT activity and odorant attraction.

Odor conditioned place preference

Odorants

We used here CITRO and LIM as attractive odorants; PYR and CRE as unattractive odorants diluted at 10Pa in mineral oil. Mineral oil served as control.

Experimental design

To avoid neophobic response, mice were exposed twice a day (one h each time) during 10 days with either CITRO (n = 8), LIM (n = 10), PYR (n = 8), CRE (n = 9) or no odor (NO; mineral oil, n = 10) before CPP test. Then, mice were all trained in CPP using the same odor as the one used for the exposure.

CPP protocol

Mice were trained in a CPP apparatus consisting of two visually different conditioning chambers (60 cm wide x 30 cm high x 30 cm long): one with orange stripes and large mesh on the wall and the other one with blue circles and short mesh on the wall, both connected by a smaller central chamber. A tea ball was placed on the top of each chamber. On day 1 (habituation), mice were allowed to move freely between the three chambers for 15 min. On day 2 (pre-conditioning test), mice had again free access to the chambers for 15 min and the time spent in the 2 conditioning chambers was video recorded using Volcan[91,92] to assess if there is a preferred chamber. Then from Day 3 to Day 7, mice were trained. Training consisted in confining the mouse alternatively in one compartment in the presence of the odorant (10μl at 10 Pa in the tea ball) and in the other compartment with no odorant (15 min per session, 4 sessions per day) in a random order. Control mice were confined alternatively in one and the other compartment with no odor in any compartment. Attractive odorants were paired to the less pleasant compartment whereas unattractive odorants were paired to the preferred compartment. At the end of the conditioning period (on Day 8), all mice have been tested without odorant, similarly to the pre-conditioning test: animals were allowed to freely explore all the chambers for 15 min and the time spent in each compartment was video recorded.

Cell assessment

VTA and OT activities were assessed with respectively TH/c-Fos and DARPP-32/c-Fos immunohistochemistry performed and analyzed as previously described.

Statistics

For each experimental group, a CPP score was calculated (time in second spent in the odor paired compartment during post conditioning – pre conditioning) to determine the effect of odor conditioning on place preference.[24] Average scores were calculated within each experimental group. One-Tailed One-Sample t-tests were used to compare CPP score to 0 (meaning no time variation between the pre and the post conditioning). One-Tailed Unpaired t-tests were used for VTA and OT activities between group comparisons.

D1 receptor blockade during CPP

CPP protocol

To determine the implication of the dopaminergic system during odor CPP, 10 mice have been injected with a specific D1 receptor antagonist (SCH23390; 0.03mg/kg intraperitoneally) 15 min before each mice confinement in the compartment containing the odorant (LIM). Saline solution has been injected 15 min before each mice confinement in the compartment containing no odor. The interval between each session was set at 2h30 to allow body elimination of the drug (half-life 40 min[90]). The protocol of CPP and its analysis were similar as previously. Another group of mice was injected with saline solution 15 min before each LIM and no odor confinement (n = 13). A last group received SCH23390 injection but without any odorant during the conditioning (n = 10).

Test of olfactory detection

Because the OB contains dopaminergic neurons, we verified that the use of dopaminergic antagonist at the dose of 0.03mg/kg does not alter olfactory detection. We thus used habituation/dishabituation paradigm (n = 8). Mice were tested on 3 trials of 2 min in which

mineral oil (no odor condition, NO) was placed in the tea ball (habituation phase); during each trial, investigation time of the tea ball was recorded (active sniffing 1cm around the tea ball, using Volcan). For the test trial (dishabituation phase), the odorant used for CPP was placed at the same concentration into the tea ball.

Locomotion test
Because dopamine is known to have an important role on locomotor activity, we analyzed the mice locomotion during 2 min, 20 min after SCH 23390 injection (n = 9) or saline injection (n = 10) using Volcan software.[91,92]

Statistics
Two-Tailed Paired t-tests were used to compare CPP score to 0. The effect of SCH-23390 on LIM detection and locomotion was assessed respectively with repeated-measure ANOVA (NO habituation effect) with Two-Tailed Paired t-test (NO3 versus LIM) and Mann-Whitney.

Conditioned place preference in humans
Conditioned place preference
Participants were told that they were going to take part in a study on the relationship between odors, emotions and learning. Experiments took place over 5 days. On the first day, participants were guided to a first room in which they were asked to perform an ETOC test to evaluate their olfactory capacities (no exclusion) and to rate their emotional state (anxious, disgusted, angry, calm, happy, arousing, scared, relaxed, stressed, and sad) using Pie-Pie software. Participants were then asked to wait in another room composed of two compartments. They were instructed to wait in this room, before a new rating test (fake survey). The aim of this new rating test was to distract participants from the CPP test that was assessed during their wait.

The CPP facility consisted in a room separated in two equal but visually different compartments equipped with webcams allowing the observation of the participant. Videos were analyzed using A2V Volcan software.[91,92] Two passive diffusers were placed in the middle of other objects on a shelf present in each compartment. On the first day (pre-conditioning test), no chair was placed in any compartment and no odor was diffused (only mineral oil placed in the diffuser). The participants were asked to wait in this room and they were allowed to visit the two compartments. Time spent in each compartment was recorded during 10 min and participant's trajectory was calculated. The next three days consisted in the conditioning phase, with 2 sessions of 10 min per day. During the conditioning phase, an odorant (50 Pa, dilution in mineral oil) was diffused in one compartment whereas no odor (mineral oil) was introduced in the diffuser of the second compartment. Note that the presence or not of the odorant was not specified to the participants. To control that the odorant was mostly perceived in the room in which the diffuser is present, we performed a preliminary experiment. In this separate experiment, after sitting for 2 min in each compartment, volunteers (n = 12) rated odorant intensity (from 1 to 9). Results indicated a highest perceived intensity in the odorized compartment (odor intensity rating: n = 12; Odorized compartment 6.000 ± 0.663 Non-odorized compartment 3.083 ± 0.583; Two-Tailed paired t-test t = 4.696 p < 0.001 Cohen's d = 1.356). The highest perceived intensity in the odorized compartment was confirmed by participants in the CPP experiment. Indeed, at the end of the experiment they were asked to rate perceived intensity and reported a significant difference in favor of the odorized compartment (odor intensity rating: n = 38; Odorized compartment 6.105 ± 0.269 Non-odorized compartment 3.579 ± 0.347; Two-Tailed paired t-test t = 6.173 p < 0.001 Cohen's d = 1.001). During the first session of the first conditioning day, participants were asked to enter in one compartment, to sit on a chair and wait. During the second session, they were asked to sit and wait in the other compartment (10 min in each compartment; odorized and non-odorized compartment were randomly presented). The order of the presented compartments (left or right) was changed every day and randomized between participants, but for a given participant, the same compartment was always paired to the odorant. The compartments were ventilated between each participant. The aim of the conditioning phase was to implicitly train participants to associate one compartment to one odorant without any instruction. The paradigm of the post-conditioning test was similar to the pre-conditioning one. No odorant and no chair were present in any compartment and participants were allowed to freely circulate in both compartments. Time spent in each compartment was recorded and participant's trajectory was analyzed.

For this experiment, three groups of 24 participants were constituted. One group performed the CPP with a compartment odorized with CAR, another group with THIO and the last group was the control group without any odorant (mineral oil) associated to any of the two compartments. Odorants were selected based on their pleasantness rating assed in a pilot study.

At the end of the last day, participants had to express their own hypothesis regarding the aim of the study. 64.2% of the participants agreed with the aim that we announced related to the effect of odors on emotions and learning. 28.4% of participants hypothesized behavioral and/or motor analyses. 7.5% hypothesized others intentions. They were also asked whether they detected an odorant during the conditioning sessions and if yes, they were asked to rate its intensity and pleasantness perception.

QUANTIFICATION AND STATISTICAL ANALYSIS

2 participants were excluded of data analyses because they were considered as outliers (superior or inferior to the means+3SD). As in mice CPP, a CPP score was calculated as the time in second spent in the odor paired compartment during post-conditioning – pre-conditioning, in order to determine the effect of odor conditioning on place preference. One-Tailed Paired t-tests were used to compare CPP score to 0. Intensity and pleasantness rating were compared between group using Mann-Whitney tests.

fMRI study
fMRI acquisition
A 3 Tesla MR-scanner was used for the experiment (AWP66012 SIEMENS Prisma). The fMRI data were collected during four sessions (285 volumes/session, interleaved, AC/AP acquisition) with a 45 axial-slice 2D EPI sequence (matrix: 78x78; TR: 2,500 ms; TE: 30 ms; FA: 90; voxel size: 2.70x2.70x2.70 mm; FOV: 270). The first seven volumes of each functional session were discarded to allow for T1 equilibration. To reduce distortion in the sinus, orbitofrontal, and temporal areas during pre-processing, a field map was acquired before fMRI data collection. For coregistration, a high-resolution T1-weighted brain image was recorded (3D MPR sequence – TR: 3500ms; TE: 3.86 ms; voxel size: 0.88x0.88x0.88 mm).

Odorants
7 odorants were selected based on previous psychophysics experiment in order to cover the entire dimension of attraction BUT, HMHA, MSH, CIS3, TER, LIM and ISO (Table S1).[31] Pure odorants (liquid) were provided by Sigma-Aldrich except for HMHA and MSH, which were synthesized for the purpose of this study, and dilutions were made using mineral oil (Sigma–Aldrich). Odor concentrations were adjusted to reach iso-intensity, using HMHA concentration as a reference. The airflow (air) was used as control condition. A computer-controlled olfactometer described in detail in Sezille et al.[93] was used to diffuse olfactory stimulation into both nostrils. The tubes were replaced every 2-3 consecutive participants.

EXPERIMENTAL PROCEDURE

An event-related design was used with 8 conditions (7 odorants + 1 clean air). The odorants were presented to participants during 5 s with 20 s interstimulus interval in 16 trials. The 8x16 trials were divided in 4 fMRI scans (sessions). For each session, the order of odorants presentation was pseudo-randomized (each of the 8 conditions were presented 4 times with no twice the same condition consecutively) and for each participant the order of sessions was pseudo-randomized. Participants were asked to breathe naturally, and odorants were diffused synchronously with the subject's nasal respiration. We chose a stimulus duration of 5 s because all the odorants were released during exhalation and had to be maintained during at least the whole duration of the subsequent inhalation (2 s). During the experiment, we recorded respiratory signal, odor valve opening and time repetition (TR) signal from the fMRI scanner, enabling event-related statistical analysis. An airflow sensor connected to a nasal cannula (Cardinal Health, OH; 2.8mm inner diameter tube) was positioned in both nostrils to measure participant's respiratory signal. A microbridge mass airflow (AWM2100V, Honey- well, MN) allowed acquisition of both inhalation and exhalation phases. Sniffing was digitally recorded at 200 Hz and stored in a computer.

   During each odorant stimulation, subjects rated odor attraction using a button-box from 1 to 5 (1 not at all attractive to 5 extremely attractive or 1 extremely attractive to 5 not at all attractive in random way). For each subject, the evaluation of all repetitions was average for each odorant.

Preprocessing
Results included in this manuscript come from preprocessing performed using FMRIPREP latest version 1.4.1[74]; RRID:SCR_016216), a Nipype[75]; RRID:SCR_002502) based tool. Each T1w (T1-weighted) volume was corrected for INU (intensity non-uniformity) using N4BiasFieldCorrection v2.1.0[77] and skull-stripped using antsBrainExtraction.sh v2.1.0 (using the OASIS template). Spatial normalization to the ICBM 152 Nonlinear Asymmetrical template version 2009c,[94] RRID:SCR_008796) was performed through nonlinear registration with the antsRegistration tool of ANTs v2.1.0,[76] RRID:SCR_004757), using brain-extracted versions of both T1w volume and template. Brain tissue segmentation of cerebrospinal fluid (CSF), white-matter (WM) and gray-matter (GM) was performed on the brain-extracted T1w using fast[95] (FSL v5.0.9, RRID:SCR_002823).

   Functional data were slice time corrected using 3dTshift from AFNI v16.2.07,[96] RRID:SCR_005927] and motion corrected using mcflirt (FSL v5.0.9; Jenkinson et al., 2002). Distortion correction was performed using fieldmaps processed with fugue[97] (FSL v5.0.9). This was followed by co-registration to the corresponding T1w using boundary-based registration[98] with six degrees of freedom, using flirt(FSL). Motion correcting transformations, field distortion correcting warp, BOLD-to-T1w transformation and T1w-to-template (MNI) warp were concatenated and applied in a single step using antsApplyTransforms (ANTs v2.1.0) using Lanczos interpolation.

   Physiological noise regressors were extracted applying CompCor.[99] Principal components were estimated for the two CompCor variants: temporal (tCompCor) and anatomical (aCompCor). A mask to exclude signal with cortical origin was obtained by eroding the brain mask, ensuring it only contained subcortical structures. Six tCompCor components were then calculated including only the top 5% variable voxels within that subcortical mask. For aCompCor, six components were calculated within the intersection of the subcortical mask and the union of CSF and WM masks calculated in T1w space, after their projection to the native space of each functional run. Frame-wise displacement[100] was calculated for each functional run using the implementation of Nipype.

   Many internal operations of FMRIPREP use Nilearn,[73] SCR_001362 principally within the BOLD-processing workflow. For more details of the pipeline see https://fmriprep.readthedocs.io/en/latest/workflows.html.

Statistical analysis
Before statistical analysis preprocessed functional images were smoothed ($8 \times 8 \times 8 \ mm^3$ FWHM Gaussian kernel) to take account of between-subject anatomical variation. Statistical analysis used SPM12 software (Statistical Para- metric Mapping; Welcome

Current Biology
Article

 CellPress

Department of Cognitive Neurology, London, UK) implemented with MATLAB 9.4 (r2018a, Mathworks). The first-level statistical analysis was modeled using a canonical hemodynamic response function. Eights regressors of interest were included in the model corresponding to the eight conditions. Motion parameters (3 rotations, 3 translations), frame displacement, 6 aCompCor components, a discrete cosine transform basis set acting as high-pass filter (with 128 s cutoff) and nasal respiration signal were also included in the model as regressors of no interest. For nasal respiration signal, before it was included as covariate, the raw signal (200Hz) was downsampled into the fMRI frequency (1/RT) using the Fourier method implemented in the "resample" function from Scipy software (Python Library). Finally, for each subject, the seven contrast of interest consisted in comparing each of the odor condition with the "air" condition.

Here we used fMRI to investigate patterns of activity in olfactory areas. For this purpose, we conducted region of interest (ROI) approach because of the important anatomical variability in these areas. The neural activity (mean signal (β) amplitude) in the OT, aPirCX and pPirCX were extracted for each contrast of interest (BUT versus air, HMHA versus air, MSH versus air, CIS3 versus air, TER versus air, LIM versus air and ISO versus air) and each participant. PirCX has already been investigated in humans, so we used standard preexisting templates. Studies on the OT are more rare, only one group has clearly studied it.[42,101] Therefore, based on these publications and using the May Atlas (May, 2014) as a support, we drew individually each region of interest using MRIcron software (https://people.cas.sc.edu/rorden/mricron/index.html).Each region was drawn individually for each participant from coronal slices in both hemispheres before functional analysis and thus any error was unrelated to functional condition. Mean images and binary masks were calculated using Imcalc in SPM. To keep a voxel in the binary mask, at least 30% of subjects had to have the voxel in their ROI. For OT, aPirCX and pPirCX, brain activity of both hemispheres were averaged.

To test whether odorant attraction modulate OT activity, we formed for each subject a group of "attractive odorants" and a group of "unattractive odorants" based on odorant attraction evaluation collected during MRI (attractive and unattractive for odorants rated $\geq$ 3 and < 3 respectively). Since, one odorant can be considered as pleasant for one subject (attraction $\geq$ 3) while it is not for another (attraction < 3), we formed the attraction-based odorant groups for each subject for tacking account of inter individual variability in attraction ratings.

We used repeated-measure ANOVA for hemisphere*attraction interaction analyses and compared brain activity in respond to attractive versus unattractive odorants using Bonferroni corrected One-Tailed Paired t-tests.

QUANTIFICATION AND STATISTICAL ANALYSIS

All statistical analyses were performed using Statistica. Kolmogorov-Smirnov test was used to assess normality of the data and variance was assessed using Levene test and parametric or non-parametric tests were performed according to that. One-Tailed tests were performed when an assumption about the direction of the variation from a reference value was made; otherwise Two-Tailed tests were used. Bonferroni corrections were performed for multiple comparisons. Significant result was set at $p < 0.05$. No statistical methods were used to predetermine sample sizes, but our sample sizes were similar to those reported in previous publications.[6,102–105] Effect size were calculated using Cohen's d and Rank-Biserial Correlation for parametric and non-parametric tests respectively. In addition, fMRI statistical analysis used SPM12 software (Statistical Parametric Mapping; Welcome Department of Cognitive Neurology, London, UK) implemented with MATLAB 9.4 (r2018a, Mathworks). Statistical tests used can be found in the star methods and result sections. The exact value of n as well as the precision measure can be found in the figure legends. In the manuscript, n represent the number of individuals or mice depending on the experiment.